2005-12

Inlet flow-field measurements of a transonic compressor rotor prior to and during steam-induced rotating stall

Payne, Thomas A.

Monterey, California. Naval Postgraduate School

NAVAL POSTGRADUATE SCHOOL

MONTEREY, CALIFORNIA

THESIS

INLET FLOW-FIELD MEASUREMENTS OF A TRANSONIC COMPRESSOR ROTOR PRIOR TO AND DURING STEAM-INDUCED ROTATING STALL

by

Thomas A. Payne

December 2005

Thesis Advisor:	Garth V. Hobson
Second Reader:	Raymond P. Shreeve

THIS PAGE INTENTIONALLY LEFT BLANK

REPORT DOCUMENTATION PAGE			Form Approved OMB No. 0704-0188
Public reporting burden for this collection of information is estimated to average 1 hour per response, including the time for reviewing instruction, searching existing data sources, gathering and maintaining the data needed, and completing and reviewing the collection of information. Send comments regarding this burden estimate or any other aspect of this collection of information, including suggestions for reducing this burden, to Washington headquarters Services, Directorate for Information Operations and Reports, 1215 Jefferson Davis Highway, Suite 1204, Arlington, VA 22202-4302, and to the Office of Management and Budget, Paperwork Reduction Project (0704-0188) Washington DC 20503.			
1. AGENCY USE ONLY ***(Leave blank)***	**2. REPORT DATE** December 2005	**3. REPORT TYPE AND DATES COVERED** Master's Thesis	
4. TITLE AND SUBTITLE: Inlet Flow-Field Measurements of a Transonic Compressor Rotor Prior to and During Steam-Induced Rotating Stall			**5. FUNDING NUMBERS**
6. AUTHOR(S) Thomas A. Payne			
7. PERFORMING ORGANIZATION NAME(S) AND ADDRESS(ES) Naval Postgraduate School Monterey, CA 93943-5000			**8. PERFORMING ORGANIZATION REPORT NUMBER**
9. SPONSORING /MONITORING AGENCY NAME(S) AND ADDRESS(ES) N/A			**10. SPONSORING/MONITORING AGENCY REPORT NUMBER**
11. SUPPLEMENTARY NOTES The views expressed in this thesis are those of the author and do not reflect the official policy or position of the Department of Defense or the U.S. Government.			
12a. DISTRIBUTION / AVAILABILITY STATEMENT Approved for public release; distribution is unlimited			**12b. DISTRIBUTION CODE**

13. ABSTRACT (maximum 200 words)

Steam leakage from an aircraft carrier catapult is sometimes ingested by the aircraft's engines upon launch which may induce compressor stall. Investigation of the phenomenon known as a "pop stall" is of particular importance as the Navy prepares to field the F35C, the aircraft carrier variant of the joint strike fighter. The single engine design of the F-35C makes this aircraft particularly susceptible to steam-induced stall during catapult launch. The present project examined compressor stall and included steady-state as well as transient measurements in the inlet of a transonic compressor prior to and during a steam-induced stall. Hotwire measurements of the inlet flow field were taken to determine an inlet turbulence intensity of 2-3% during both subsonic as well as transonic compressor operation. A 95% speed line was established from data taken from open throttle to near stall. Hot-film and Kulite pressure data taken near stall showed the existence of a stall precursor which appeared near half rotor speed. Steam was injected into the inlet; however the initial method added mass to the system and did not induce a stall. A decrease in the amplitude of the pressure trace was observed however. A stall was induced by steam ingestion ahead of the existing inlet throttle, with upstream transient measurements taken using both hot-film and Kulite pressure transducers.

14. SUBJECT TERMS Compressor, Transonic, Steam Ingestion, Turbulence, Stall			**15. NUMBER OF PAGES** 87
			16. PRICE CODE
17. SECURITY CLASSIFICATION OF REPORT Unclassified	**18. SECURITY CLASSIFICATION OF THIS PAGE** Unclassified	**19. SECURITY CLASSIFICATION OF ABSTRACT** Unclassified	**20. LIMITATION OF ABSTRACT** UL

NSN 7540-01-280-5500 Standard Form 298 (Rev. 2-89)
Prescribed by ANSI Std. 239-18

THIS PAGE INTENTIONALLY LEFT BLANK

Approved for public release; distribution is unlimited

INLET FLOW-FIELD MEASUREMENTS OF A TRANSONIC COMPRESSOR ROTOR PRIOR TO AND DURING STEAM-INDUCED ROTATING STALL

Thomas A. Payne
Lieutenant, United States Navy
B.S., Rensselaer Polytechnic Institute, 2000

Submitted in partial fulfillment of the
requirements for the degree of

MASTER OF SCIENCE IN MECHANICAL ENGINEERING

from the

NAVAL POSTGRADUATE SCHOOL
December 2005

Author: Thomas A. Payne

Approved by: Garth V. Hobson
Thesis Advisor

Raymond Shreeve
Second Reader

Anthony Healey
Chairman, Department of Mechanical and Astronautical Engineering

THIS PAGE INTENTIONALLY LEFT BLANK

ABSTRACT

Steam leakage from an aircraft carrier catapult is sometimes ingested by the aircraft's engines upon launch which may induce compressor stall. Investigation of the phenomenon known as a "pop stall" is of particular importance as the Navy prepares to field the F35C, the aircraft carrier variant of the joint strike fighter. The single engine design of the F-35C makes this aircraft particularly susceptible to steam-induced stall during catapult launch. The present project examined compressor stall and included steady-state as well as transient measurements in the inlet of a transonic compressor prior to and during a steam-induced stall. Hotwire measurements of the inlet flow field were taken to determine an inlet turbulence intensity of 2-3% during both subsonic as well as transonic compressor operation. A 95% speed line was established from data taken from open throttle to near stall. Hot-film and Kulite pressure data taken near stall showed the existence of a stall precursor which appeared near half rotor speed. Steam was injected into the inlet; however the initial method added mass to the system and did not induce a stall. A decrease in the amplitude of the pressure trace was observed however. A stall was induced by steam ingestion ahead of the existing inlet throttle, with upstream transient measurements taken using both hot-film and Kulite pressure transducers.

THIS PAGE INTENTIONALLY LEFT BLANK

TABLE OF CONTENTS

LIST OF FIGURES

LIST OF TABLES

THIS PAGE INTENTIONALLY LEFT BLANK

ACKNOWLEDGMENTS

I could not have chosen a better learning environment than the Turbopropulsion Laboratory. I would like to thank Professor Hobson for unbelievable amount of effort he put forth in order to help me complete this thesis. His reputation for being the hardest working professor on campus is well deserved and appreciated by his thesis students. I would like to thank Professor Shreeve for his patience and encouragement. I would also like to thank John and Rick. Not only are the day to day operations of the lab made possible because of their efforts, but their friendly dispositions always made the lab an enjoyable place to be.

THIS PAGE INTENTIONALLY LEFT BLANK

I. INTRODUCTION

The catapult-launch systems on today's aircraft carriers are known to release steam during the launch cycle, especially as the seals degrade over time. When this steam is ingested into the intakes of aircraft, it can cause a phenomenon known as "pop stall" causing a loss of power and possible total engine stall. Experiments with an F-18 conducted at Lakehurst Naval Engineering Station (Figure 1) demonstrated the susceptibility of current aircraft to steam induced stall.

Figure 1. F-18 "Pop-Stall" during Lakehurst steam ingestion experiment

This phenomenon is of particular concern to the Navy as it prepares to transition to the single engine F-35C, the carrier variant of the Joint Strike Fighter (JSF). The single engine design of this aircraft increases the probability of a pop stall resulting in catastrophic loss of the aircraft.

The focus of the work conducted at the Turbopropulsion Laboratory (TPL) at the Naval Postgraduate School (NPS) is concentrated on the "pop-stall" problem. Investigations conducted with the Transonic Compressor Rig (TCR) are intended to improve the understanding of the nature of steam induced stall. The present transonic compressor fan stage was designed specifically for the Naval Postgraduate School to be used in their TCR by Sanger (1996) at the NASA Glenn Research Center (Ref. 1 and 2).

Extensive amounts of data were collected by Gannon, Hobson and Shreeve in order to map the performance characteristics of the compressor in both the fan-stage as well as rotor-only configurations. The data were used to investigate the conditions of the TCR prior to and during stall as well as establish performance characteristics at 70%, 80%, 90% and 100% design speed. (Ref. 3-5)

Unsteady pressure measurements at 60%, 70%, and 80% design speed were reestablished by Rodgers in 2003 (Ref. 6). Villescas conducted inlet and exit surveys at 70%, 80%, 90% and 100% design speed with a three-hole probe and determined spanwise distributions of the rotor diffusion factor at choke, peak efficiency and stall (Ref. 7). Brunner repeated Villescas' inlet flow-field surveys with a five-hole probe and determined pitch angle and Mach number distributions in the inlet to the rotor (Ref. 8).

The present experiment furthered the understanding of the performance characteristics of the transonic compressor rotor prior to and during steam-induced stall. Turbulence intensity measurements were taken upstream of the rotor in order to characterize the inlet flow conditions, as well as to document the inlet turbulence for future computational fluid dynamics (CFD) simulations. Performance measurements were taken at 95 percent speed from open throttle to near stall, and the data were added to the existing compressor map. Data taken upstream of the rotor at 90% speed by both a hot-film probe as well as Kulite pressure transducers in the case wall were analyzed to determine stall precursor events. Finally, transient data were collected from both the hot-film as well as Kulite pressure transducers during steam induced stall at 70% speed.

II. EXPERIMENTAL FACILITY AND EQUIPMENT

The present study was conducted at the Turbopropulsion Laboratory (TPL) within the Department of Mechanical and Astronautical Engineering a the Naval Postgraduate School (NPS).

A. TRANSONIC COMPRESSOR

The Transonic Compressor Rig (TCR), as shown in Figure 2, was driven by two opposed-rotor air turbine stages, supplied by an Allis-Chalmers axial compressor. The Allis-Chalmers compressor supplied three atmospheres of air pressure at a mass flow rate of 5 kg/s. The configuration tested was detailed extensively by O'Brien (Ref. 9) and Papamarkos (Ref. 10).

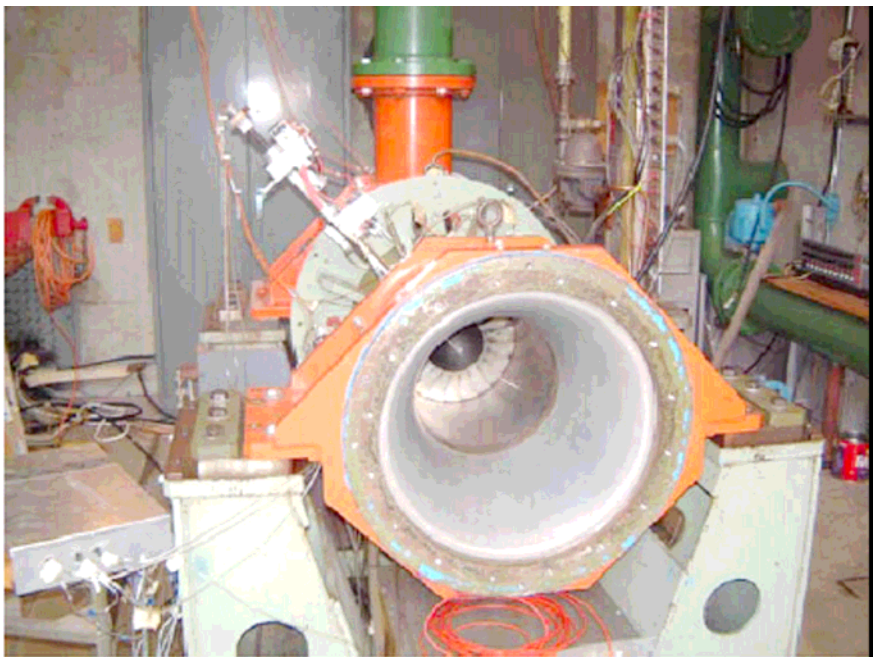

Figure 2. Transonic compressor rig in test cell with inlet piping removed.

The transonic compressor rotor, was designed as part of a complete fan stage by Sanger using a CFD code (Ref. 1). By employing numerical machining, the stage was manufactured specifically for testing and evaluation within the TCR.

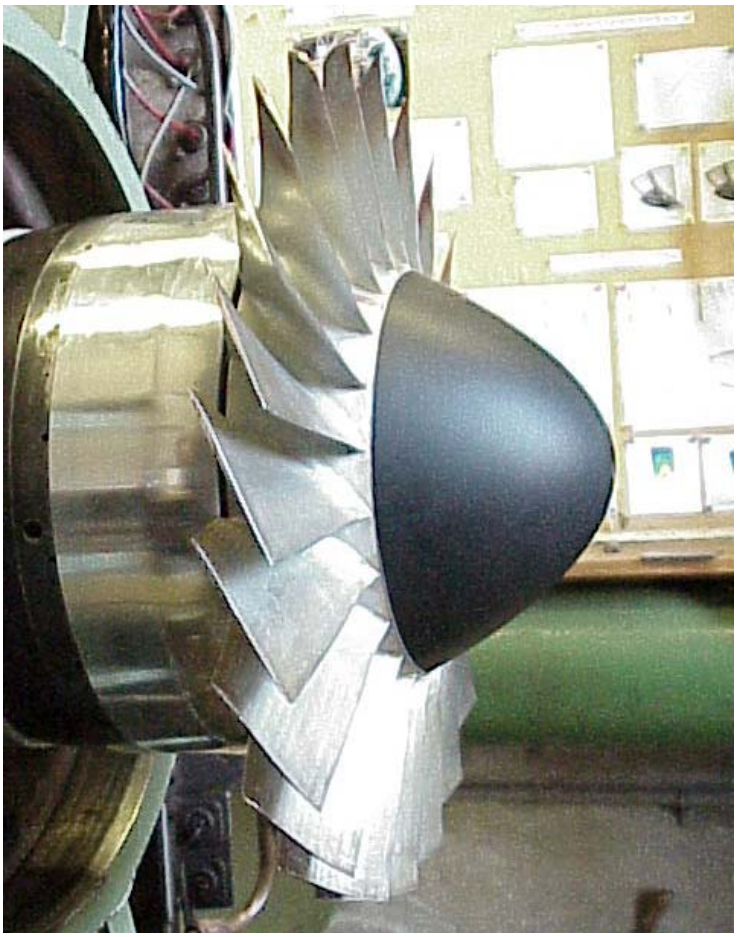

Figure 3. As tested rotor only configuration.

The rotor had 22 blades and was made from a high strength aluminum alloy (7075-T6). In the present experiment, the rotor was tested with a parabolic spinner, which replaced the conical spinner used by O'Brien (Ref. 9).

In most of the previous studies the entire stage was evaluated. In the present experiments, the stator was removed and only the rotor was present. This was to use the simplest configuration during the initial steam ingestion experiments. Table 1 below was reproduced from Sanger's "Design Methodology" (Ref. 1) and details the design parameters for the rotor.

Table 1. Sanger rotor design parameters (Ref 1)

Parameter	Value
Pressure Ratio	1.61
Tip Speed	33.02 m/s (1300ft/s)
Design Speed	27085 rpm
Design Mass Flow	7.75 kg/s (17.05lb/s)
Specific Mass Flow	170.88 kg/s-m^2 (35lbm/s-ft^2)
Specific Head Rise	.246
Tip Inlet Relative Mach Number	1.28
Aspect Ratio	1.2
Hub/Tip Radius Ratio	.51
Rotor Inlet Ramp Angle	28.2
Number of Rotor Blades	22
Tip Solidity (Rotor)	1.3
Outside Diameter	0.2794m (11 inches)
Rotor Diffusion Factor – Tip	.4
Rotor Diffusion Factor - Hub	.47

B. STEAM INGESTION/COMPRESSOR SYSTEM

The steam generator used in the present experiment, as seen in Figure 4, was a Sussman model SVS600 steam boiler. The SVS600 was capable of producing saturated steam up to a maximum working pressure of 1000 kPa or 1.4 kg/sec at 100C. (Ref. 11)

Figure 4. Sussman model SVS600 steam boiler.

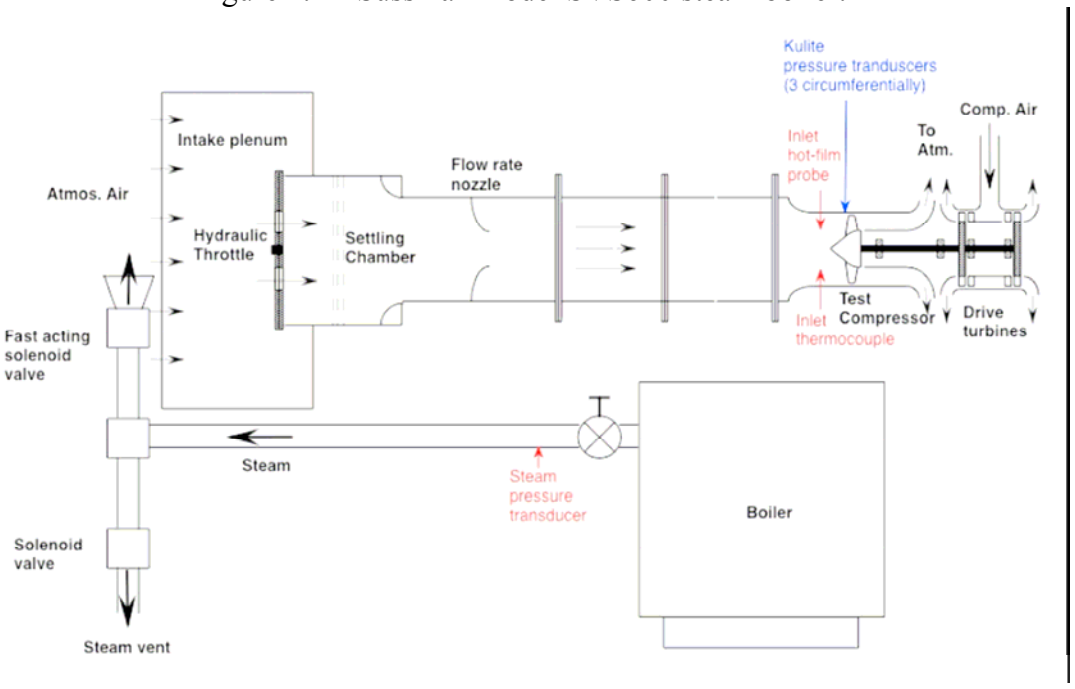

Figure 5. Steam ingestion/compressor system

The layout of the compressor rig and steam ingestion system is shown in Figure 5. Steam produced by the steam generator was directed via a 7.62 cm(three inch) diameter pipe and vented just outside the intake plenum. Figure 6 shows the orientation of the steam pipe with respect to the intake plenum. A pressure transducer was installed in the steam pipe so that the transient response of the steam pressure could be monitored. Two fast-acting, remote-operated solenoid valves were used for venting the pipe as well as releasing steam into the intake plenum.

Figure 6. Steam pipe and intake plenum orientation

Air was drawn into the compressor from atmosphere through a hydraulically operated throttle valve shown in Figure 5. A five-meter long 46cm diameter pipe connected the settling chamber to the test compressor. The pipe contained a nozzle, which was used for flow rate measurements, as well as a transition duct to the 27.94cm

case wall. A hot-film probe and a thermocouple probe were mounted in the case wall 11.5 cm upstream on the leading edge of the rotor, as shown in Figure 5.

III INSTRUMENTATION

A. PROBES

1. Hot-Film

Hot-wire anemometry measurements were taken in order to characterize the inlet-flow conditions. Measurements were taken using a 20 micron TSI model 1212-20 hot-film probe (Figure 8, Ref 12) with serial number 70536123. Data were acquired using an IFA 100 Intelligent Flow Analyzer, and TSI ThermalPro software version 4.53, running on a PC.

Figure 7. TSI model 1212-20 hot-film probe (From Ref 12)

2. Kulite Pressure Transducer

A Kulite Pressure Transducer, model XCQ-080, was used to obtain time-resolved wall pressure data. The probe was a miniature, semiconductor, strain-gauge transducer that incorporated a fully active four-arm Wheatstone bridge, which was dielectrically isolated on a silicon-on-silicon diaphragm. The natural frequency of the probe was 300 kHz. A diagram of the probe is given in Figure 8 and the factory specifications are given in Table 2.

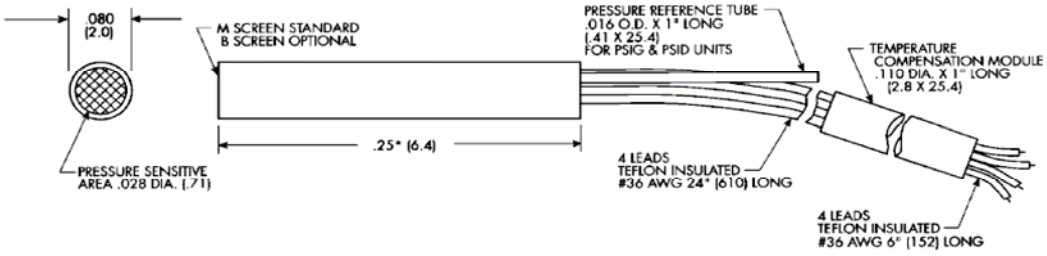

Figure 8. Kulite XCQ-080 series transducer (Ref 6)

Table 2. Factory specifications for XCQ-080 (Ref 6).

Input	
Pressure Range	25 psi
Over Pressure	50 psi
Burst	75 psi
Rated Electrical Excitation	10 VDC/AC
Maximum Electrical Excitation	15 VDC/AC
Input Impedance	800 Ohms
Output	
Output Impedance	1000 Ohms
Full Scale Output	100 mV
Residual Unbalance	+-3 % FSO
Non-Linearity and Hysterisis	0.1 % FS BFSL
Hysteresis	0.1 %
Repeatability	0.1 %
Resolution	Infinite
Natural Frequency	300 kHz
Perpendicular Accel Sensitivity	0.0003 % FS/g
Transverse Accel Sensitivity	0.00004 % FS/g
Insulation Resistance	100 Megohm
Environmental	
Operating Temp Range	-65 to 250 deg F
Compensated Temp Range	80 to 180 deg F
Thermal Zero Shift	+- 1 % FS/100 F
Thermal Sensitivity Shift	+- 1 % FS/100 F

B. INSTALLATION OF SENSORS

1. Hot-Film Probe

The hot-film probe was installed in the case wall 11.5cm upstream of the leading edge of the rotor, and extended 4cm into the flow as shown in Figure 5. As can be seen in Figure 7, the sensor needles that hold the hot-film were bent forward and in this experiment the probe was positioned so that the leads pointed into the flow. The probe holder used to secure the probe is shown in Figure 9. The relative position of the probe ahead of the rotor in the inlet casing can be seen in Figure 10.

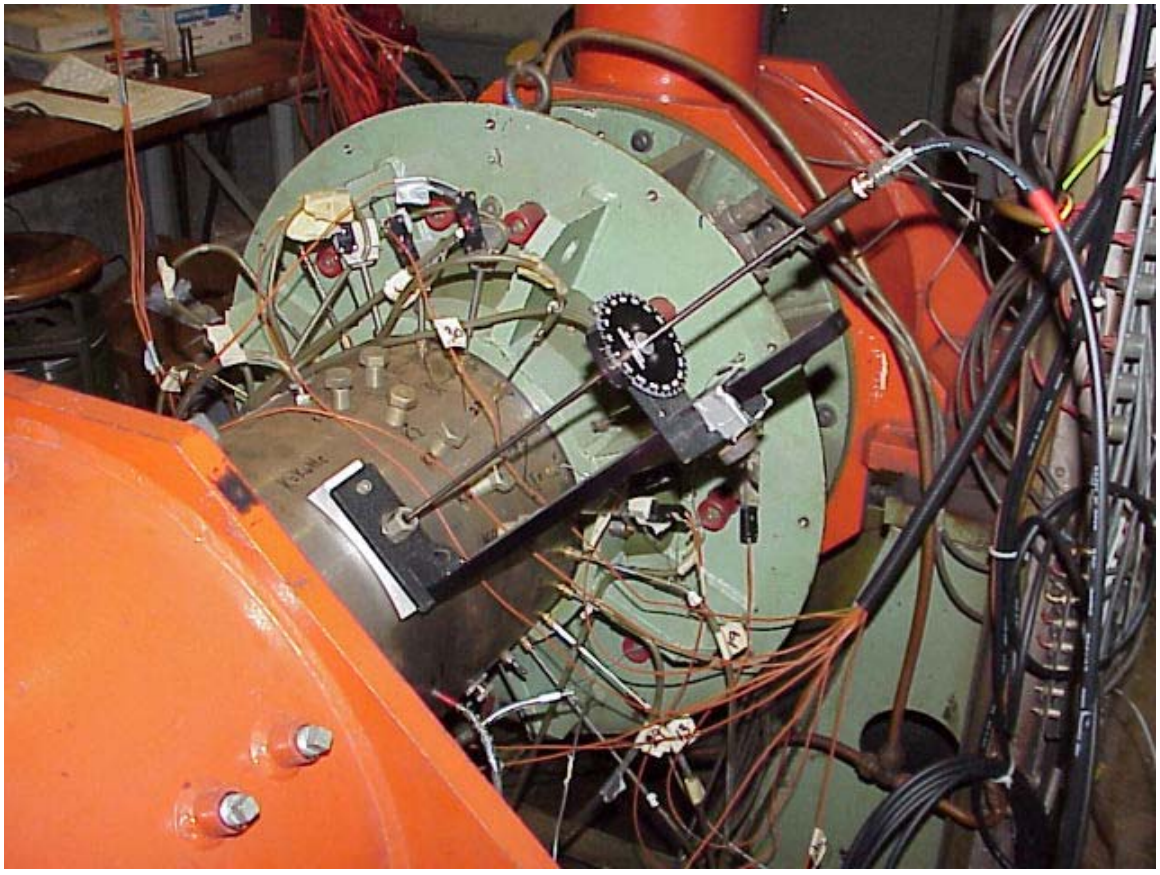

Figure 9. Hot-film probe holder installed in inlet casing

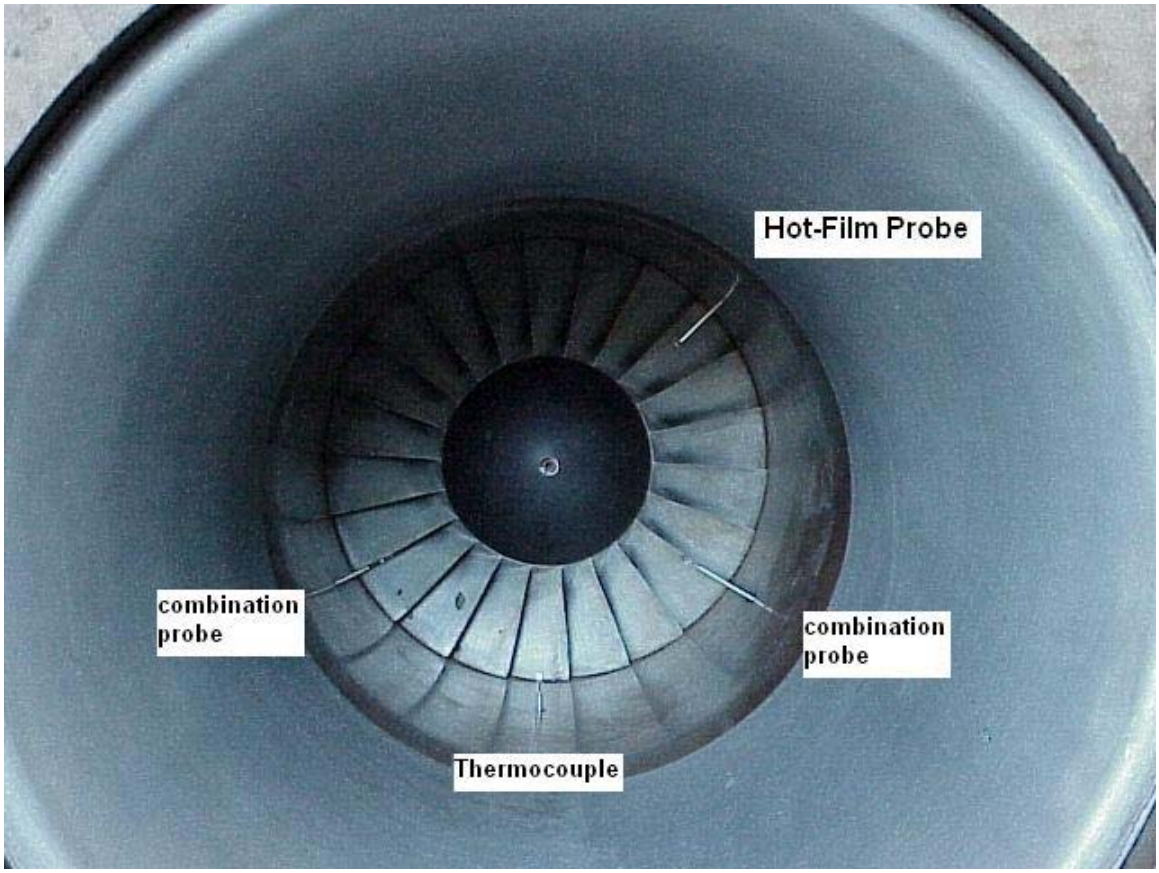

Figure 10. Relative position of hot-film probe

2. Kulite Pressure Transducers

Three Kulite pressure transducers (designated 2, 8, and 9 in Figures 11 and 12) were mounted flush with the case wall. Transducer 2 was located closest to the rotor approximately 1 cm from the leading edge just off top dead center. Transducers 8 and 9 were located 120 degrees from transducer 1 but approximately 2 cm ahead of the rotor.

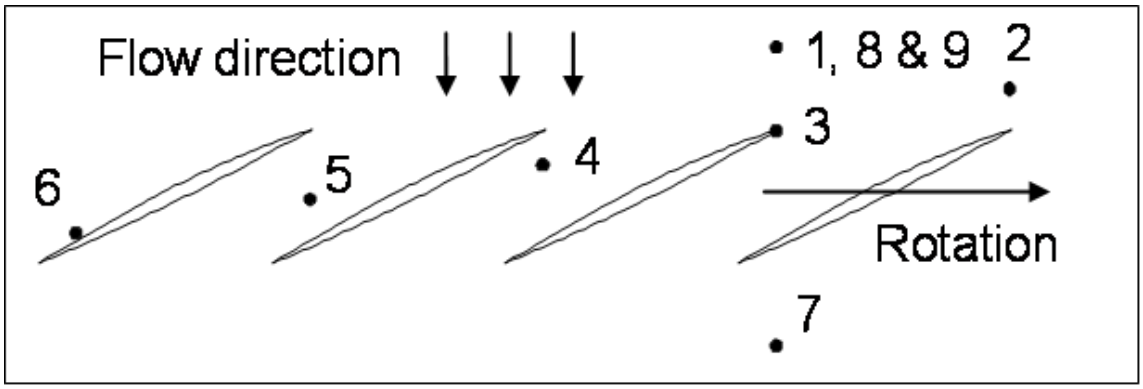

Figure 11. Relative positions of Kulite pressure transducer and blades. (From Ref 6)

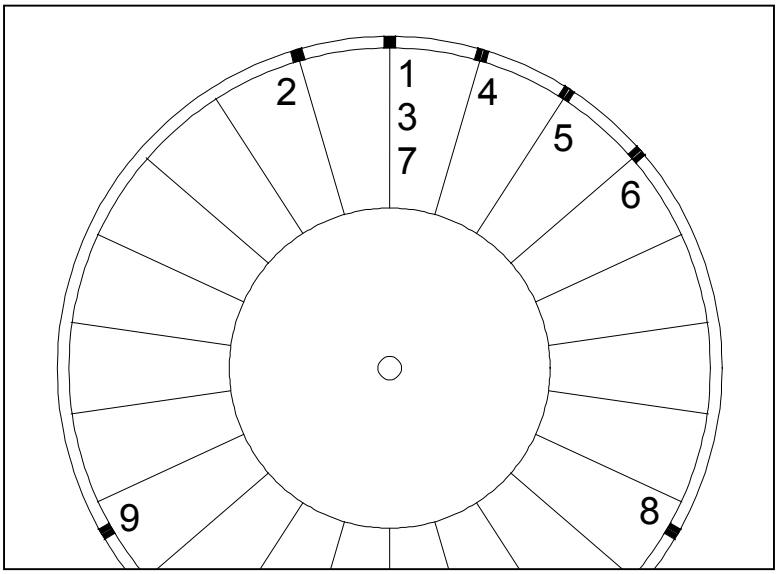

Figure 12. Relative positions or Kulite pressure transducers in case wall (From Ref 6)

C. DATA ACQUISITION

1. Hot-Film Data Acquisition

Figure 13 shows the layout of the hot-film data acquisition system. An IFA 100 Intelligent Flow Analyzer was used for hot-film data acquisition. The probe was connected to the IFA 100 via a double-shielded coax cable. Instantaneous voltages from the anemometer were sent to a United Electronic Industries Power DAQ A/D Board Model PD2-MFS-4-1M/12 installed in the P.C. via a terminal board. Control of the IFA 100 from the PC was via an RS-232-C Digital Control Line.

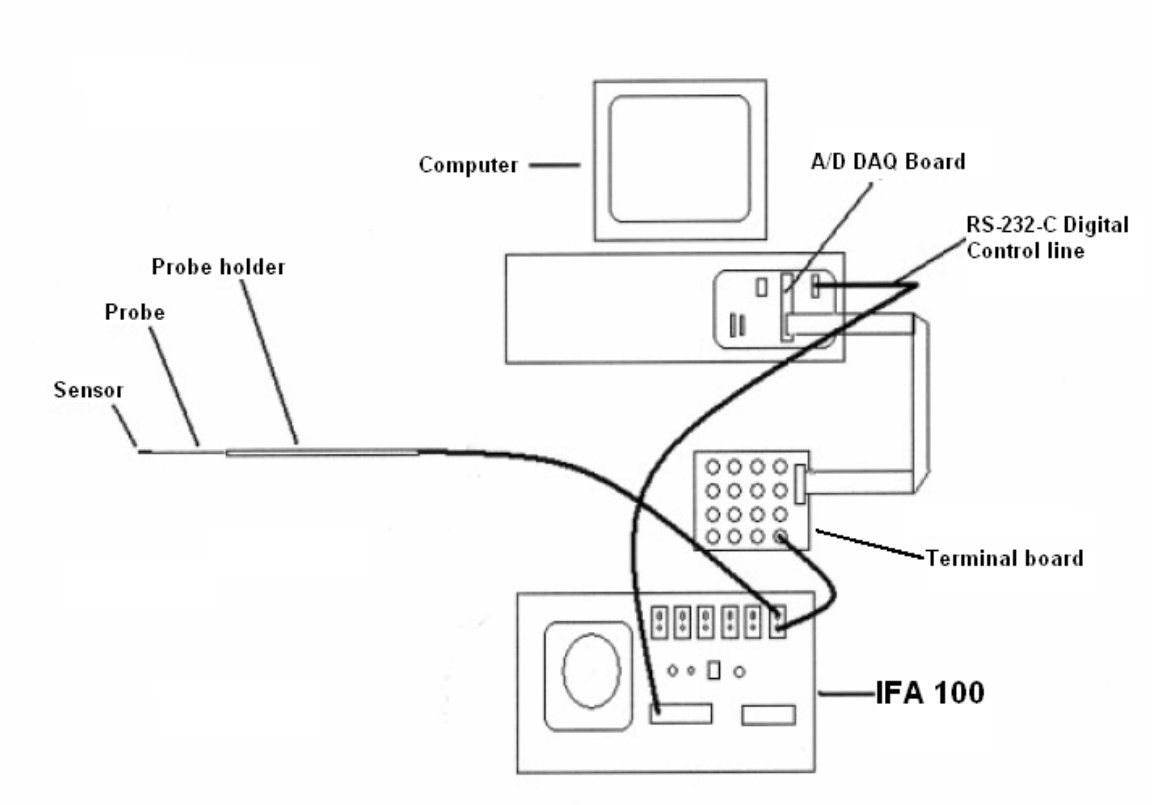

Figure 13. Hot-film data acquisition system

2. Kulite Data Acquisition

The Kulite data acquisition system is shown in Figure 14. The Kulite pressure transducer was connected to the Hewlett-Packard E1529A Remote Strain Conditioning Unit via an RJ-45 LAN cable. Also connected to the Hewlett-Packard E1529A was a two channel power supply used to meet the 5 volt bridge excitation requirement of the Kulites. The HP E1529A was connected to the data interface port of the HP E1422A via an RJ-45 cable. The HP E1529A was connected to the HP E1433A digitizer via a 37-pin connection. A tachometer signal was connected to the HP E1433A in order to provide a speed reference to the data. Also connected to the HP E1433A was the signal from the IFA 100. This allowed for easy time-based comparison of the hot-film data and the Kulite data. Both the IFA 100 signal as well as the tachometer signal came in via standard coax cables and a break-out box was used as an adapter to route these signals into the 27 pin connection of the HP E1433A. The HP E1433A and HP E1422A were

addressed through the HP E8404A VXI Mainframe and interfaced to a PC. A full description of the Kulite data acquisition system was given by Rodgers (Ref. 6).

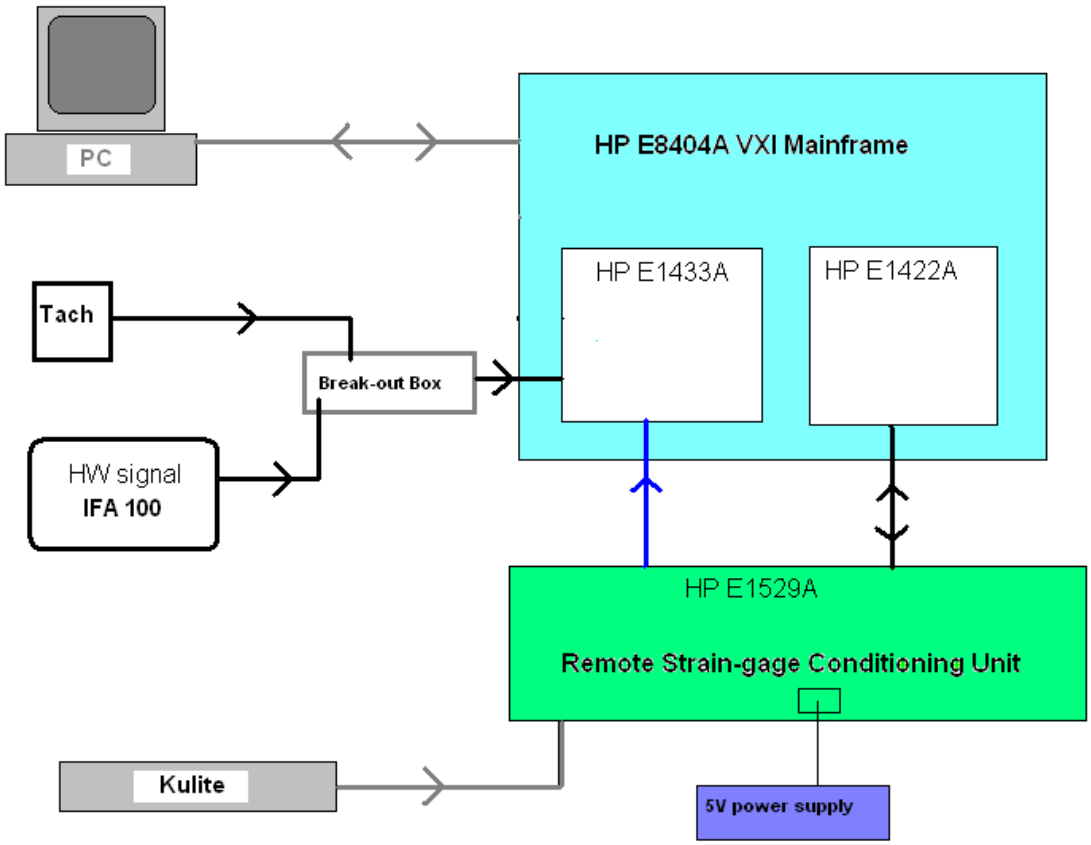

Figure 14. Kulite data acquisition system

THIS PAGE INTENTIONALLY LEFT BLANK

IV. EXPERIMENTAL PROCEDURE

A. PROBE AND TRANSDUCER CALIBRATION

Calibration of the hot-film probe was conducted in situ. After inserting a shorting probe in the place of the hot film probe, the cable resistance was measured using the IFA 100. After replacing the shorting probe with the hot-film probe, the probe resistance was measured. Operating resistance and bridge compensation was set according to manufacturer specifications, which were probe specific. The low and high flow voltage was measured with the compressor running at 30% and100% speed. The compressor speed was then returned to 30% and increased incrementally as measurements were taken. With each hot-film measurement, the static to stagnation pressure difference was entered into the ThermalPro software for a velocity calculation. After all of the calibration measurements were taken, the ThermalPro software applied a curve fit to the calibration data and King's Law coefficients were calculated. A complete description of the calibration procedures can be found in Appendix A.

Calibration of the Kulite was carried out while the compressor was running, by applying different reference pressures to the reference tube, (Figure 8) and averaging the voltage recorded by the data acquisition system. The temperature dependence of the Kulite was alleviated by calibrating while online. A detailed account of the calibration procedure is given by Rodgers (Ref. 6).

B. TYPICAL COMPRESSOR OPERATION

Standard operating procedure for testing the TCR was to maintain a constant rotor speed while taking measurements at different throttle settings. By closing the throttle, the mass flow rate was reduced and the rig operating point could be determined by the procedures described by Gannon et al. (Ref. 6).

The first step was to open the throttle and adjust the rotor RPM to the desired speed. Table 3 is a list of typical rotor speed settings. Measurements were then taken with the rotor speed constant and the mass flow rate varied by actuating the hydraulic throttle (Figure 5). Mass flow rate, inlet and exit total temperatures and pressures were

measured to calculate total-to-total pressure ratio and isentropic efficiency in order to determine the position on the compressor performance map. Measurement and calibration procedures were described in more detail by Gannon et al. (Ref. 3). Along each speed line, measurements were taken from full open throttle to near stall.

Table 3. TCR speed settings

RPM	Percent Speed
27,085	100
25,730	95
24,376.5	90
21,668	80
18,959.5	70

C. HOT-FILM MEASUREMENTS AT 70, 90, AND 95 PERCENT SPEED

Data at 70, 90, and 95 percent speed were obtained in order to characterize the turbulence intensity levels of the inlet flow field. Data were recorded at a sampling rate of 100,000 Hz from the probe. The duration of each measurement sample was 0.0410 seconds, and contained 4096 values. Three data samples were collected at 70 percent speed at open throttle, peak efficiency, and near stall. At 90 and 95 percent speed, data were taken over the whole operating range from open throttle to near stall.

At 90 percent speed, several measurements were also made with the hot-film probe for a longer sample time. Specifically, the sample duration was 5.2429 seconds and consisted of 524,288 data points. Full procedures for operation of the ThermalPro software are given by Brown (Ref. 13).

D. PERFORMANCE MEASUREMENTS AT 95% SPEED

The procedure for creating the 95 percent speed line was similar to that mentioned above. The compressor was brought to 95 percent speed with the throttle completely open. Incrementally, over 16 points, the throttle was closed and mass flow rate, total to

total pressure ratio, and isentropic efficiency were measured using a procedure described by Gannon et al. (Ref 3). The compressor was throttled to a point near the expected stall point but not actually stalled in order to prevent damage to the rotor.

E. STEAM-INDUCED STALL RUNS

Measurements were conducted in order to ascertain the point at which steam ingested into the compressor would induce stall. For this part of the experiment, the compressor was initially set at 70 percent speed and peak efficiency. The throttle was then closed incrementally as measurements were taken at each setting. For each throttle setting, an initial steady-state measurement was taken prior to steam ingestion. Again, mass flow rate, total-to-total pressure ratio, and isentropic efficiency were measured in order to determine the location of the setting on the compressor map. Hot-film data samples lasting 5.2429 seconds, that consisted of 524,288 data points, were also taken. Kulite data were also collected at a rate of 196,608 Hz at sample lengths that varied from 3 to 8 seconds.

For each throttle setting, and after the steady-state measurements were taken, the following procedure was followed for steam ingestion. The boiler isolation valve and steam vent solenoid valve were both opened to allow the steam pipe to warm up. After the pipe was fully heated, the vent valve was closed and the data trace from the pressure transducer and thermocouple was started. When the pressure in the pipe reached a target pressure, the isolation valve was closed. A three second countdown commenced. At two seconds prior to start, the Kulite data acquisition was initiated. At one second prior to start, the hot-film data acquisition commenced. At the end of the countdown, the main steam valve (fast-acting solenoid valve) was opened allowing the steam to dump into the inlet plenum of the compressor. The steam was (observation showed) entrained through the throttle into the inlet by the suction of the compressor. After several seconds, all data acquisition was stopped. The whole procedure was repeated at reduced throttle settings until stall occurred when the steam was ingested by the compressor.

Post processing of the data was conducted with MATLAB (Ref. 14). Specific M-files that were used are given in Appendix C.

THIS PAGE INTENTIONALLY LEFT BLANK

V. RESULTS AND DISCUSSION

A. TURBULENCE INTENSITY MEASUREMENTS

Turbulence intensity values were calculated from hot-film data taken at 70, 90, and 95 percent speeds. These values were then plotted versus mass flow rate as seen in Figure 15.

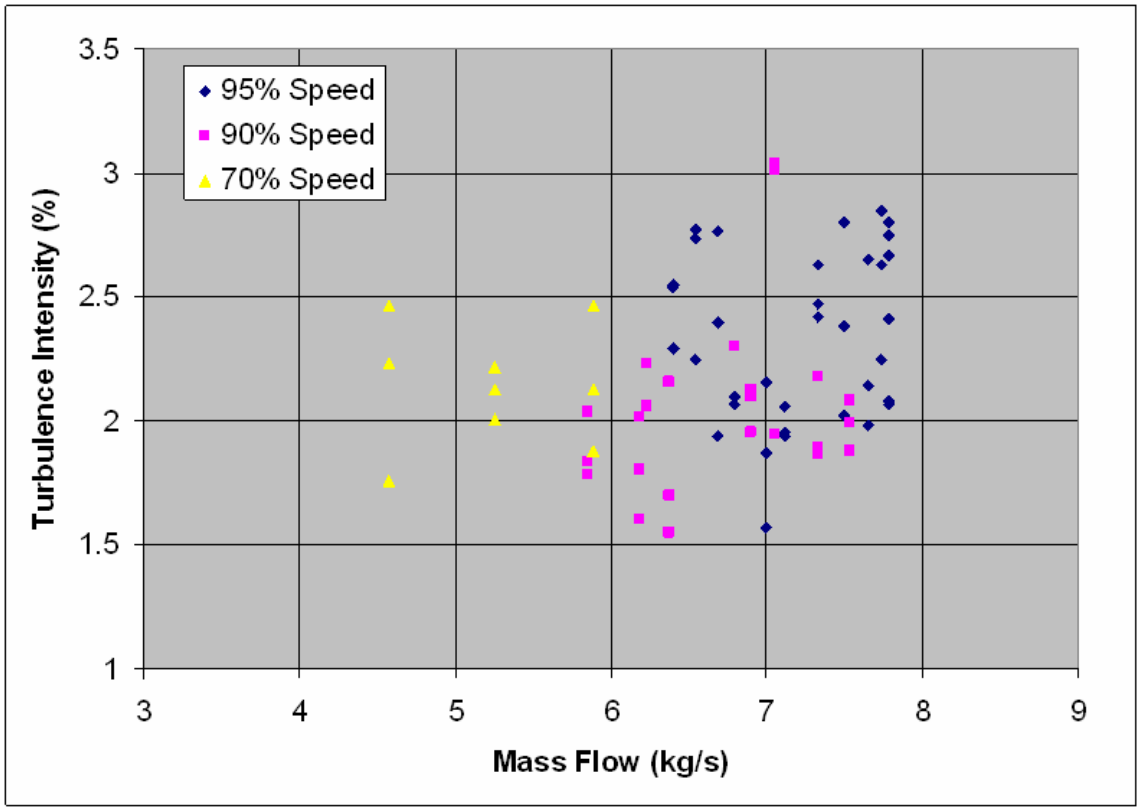

Figure 15. Turbulence intensity vs. mass flow rate

An average turbulence intensity of 2.26 percent with a variance of 0.287 was determined from these measurements. There does not appear to be a correlation between turbulence levels, and mass flow rate or speed.

B. 95% SPEED PERFORMANCE DATA

Extensive testing of the compressor was conducted by Gannon et al. at 70, 80, 90, and 100 percent speeds (Ref. 3). It was considered desirable to obtain performance data at 95 percent speed as it was comparable to cruise conditions for an actual engine. Figures 16 and 17 show the compressor performance map with the addition of the 95 percent speed line. These data closely follow those previously taken at 90 and 100 percent speed both with respect to the trend of the total pressure ratio characteristic and the value of the measured peak efficiency of 88.6 percent at 7.5kg/sec mass flow rate. The peak total-to-total pressure rise at the 95 percent speed was measured to be 1.56 at a mass flow rate of 6.5 kg/sec

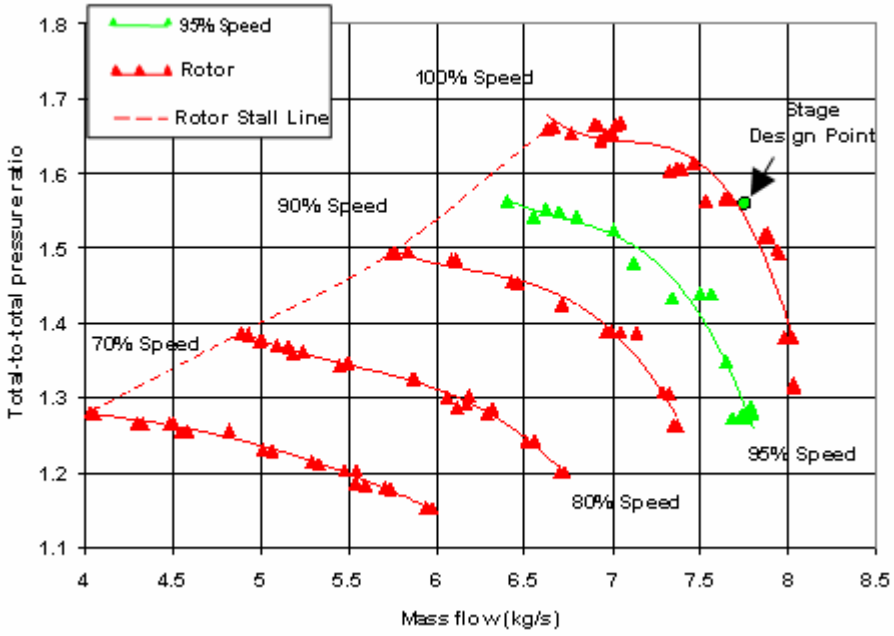

Figure 16. Pressure ratio versus mass flow rate with 95% speed line.

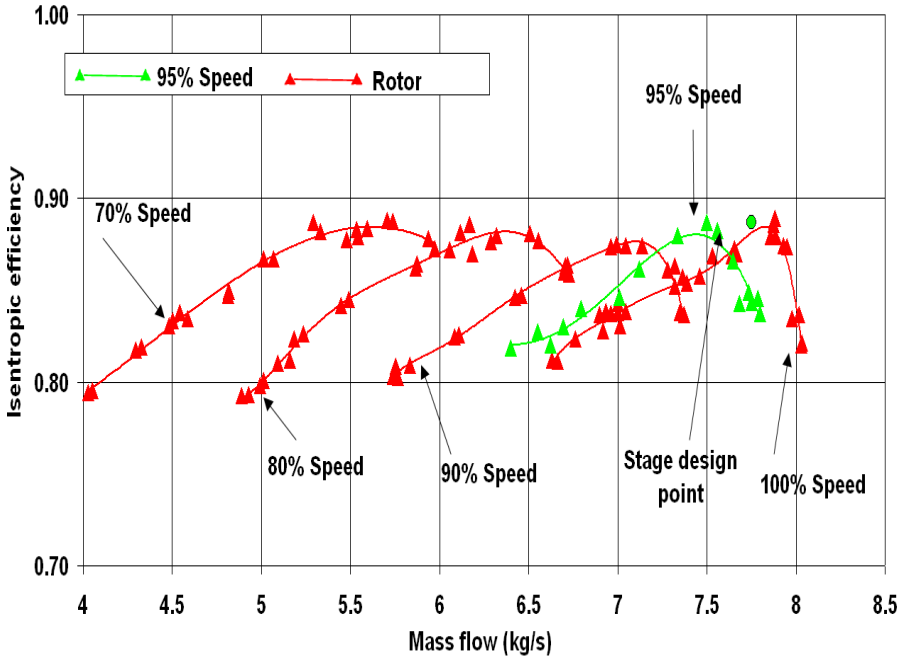

Figure 17. Isentropic efficiency versus mass flow with 95% speed line.

C. MEASUREMENTS OF STALL PRECURSOR WITH A HOT-FILM PROBE AND KULITE PRESSURE TRANSDUCERS

Figures 18 and 19 show velocity traces created from 5.2429 seconds duration hot-film data samples at 90 percent speed. The data shown in Figures 18 was taken at a mass flow rate between peak efficiency and stall at 6.5 kg/sec. Figure 19 shows data that were taken near stall at a mass flow rate of 5.75 kg/sec.

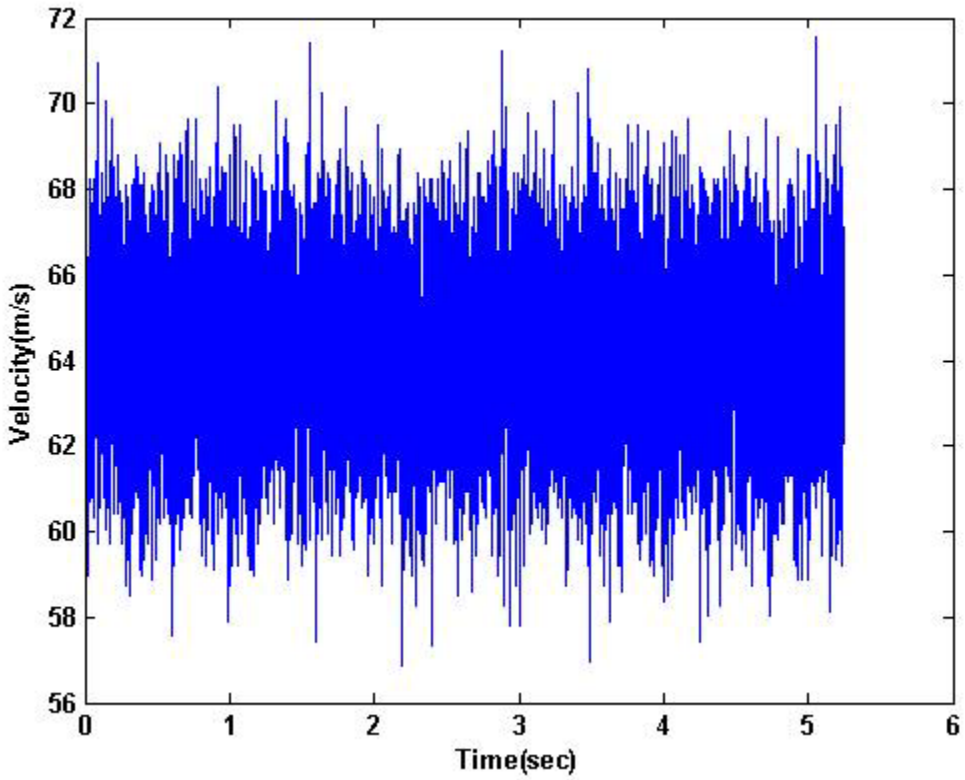

Figure 18. Instantaneous velocity trace of hot-film output at 90 percent speed between peak efficiency and stall

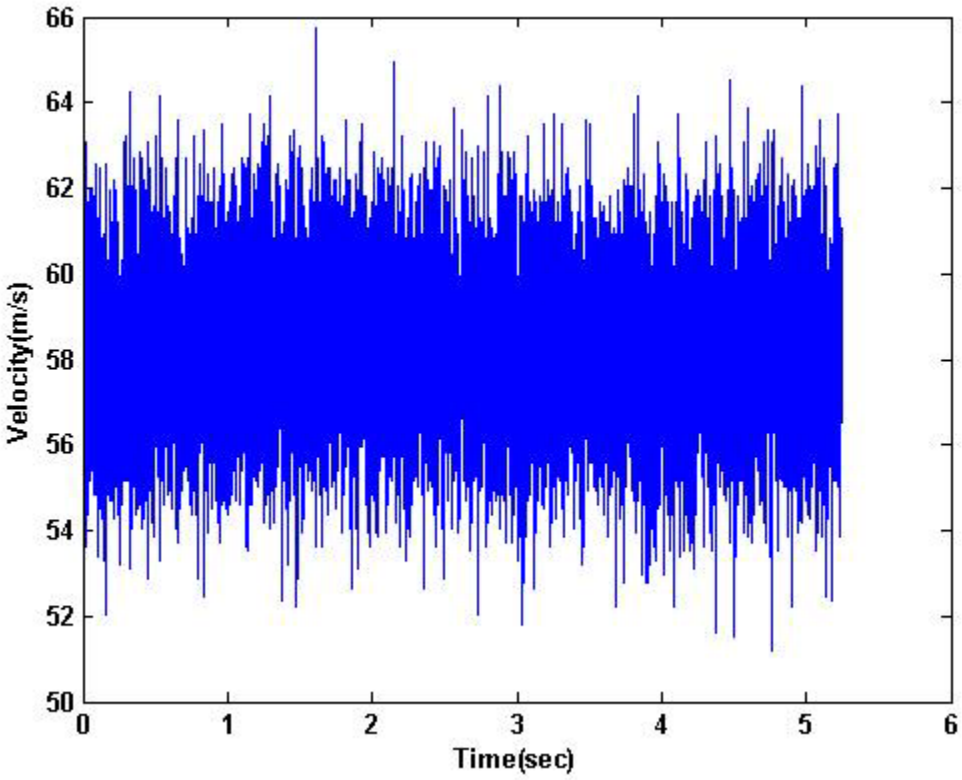

Figure 19. Velocity trace of hot-film data at 90 percent speed near stall

A power spectrum was created using a fast Fourier transform (FFT) of the hot-film data mentioned previously and the results can be seen in Figures 20 and 21. The power spectrum for the case between peak efficiency and stall shows a drop off in power level with increasing frequency, typical of free stream turbulence measurements. At a frequency of 8,938 Hz a spike occurred which corresponded to the blade-passing frequency (22 blades at 24,376 RPM).

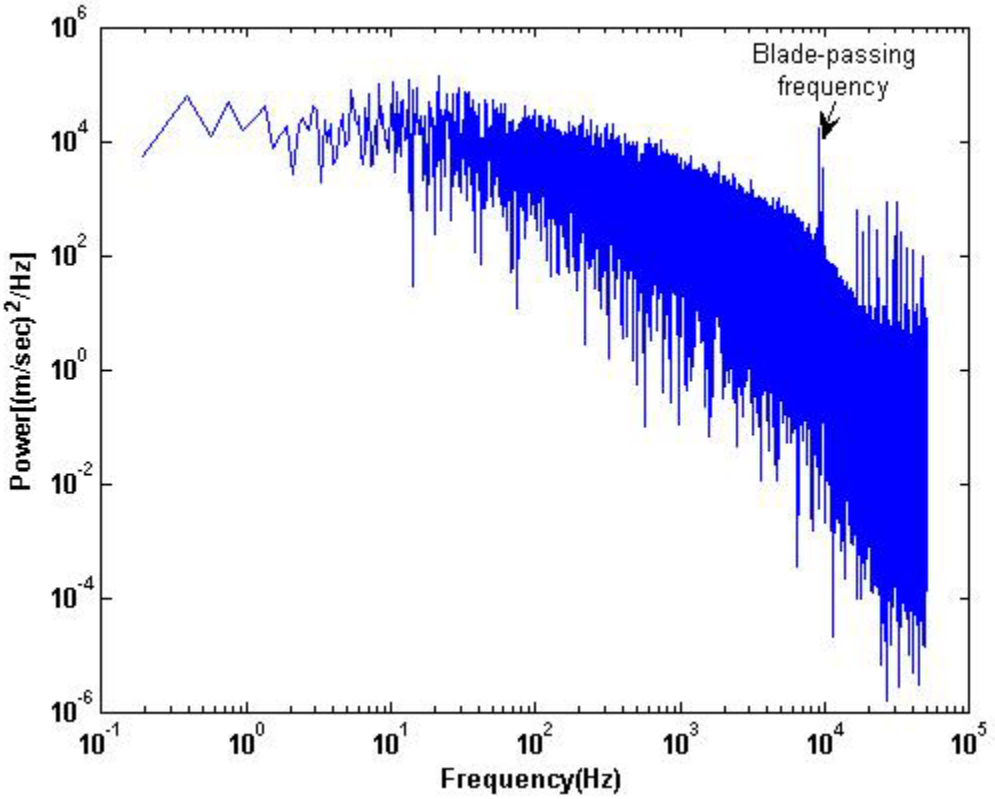

Figure 20. Power spectrum of hot-film data at 90 percent speed between stall and peak efficiency

In the FFT of the near-stall condition the same overall shape appeared with the spike at the blade-passing frequency. However there was slight evidence of the once-per-rev frequency of 406 Hz as well as an event at half this frequency, as annotated on Figure 21.

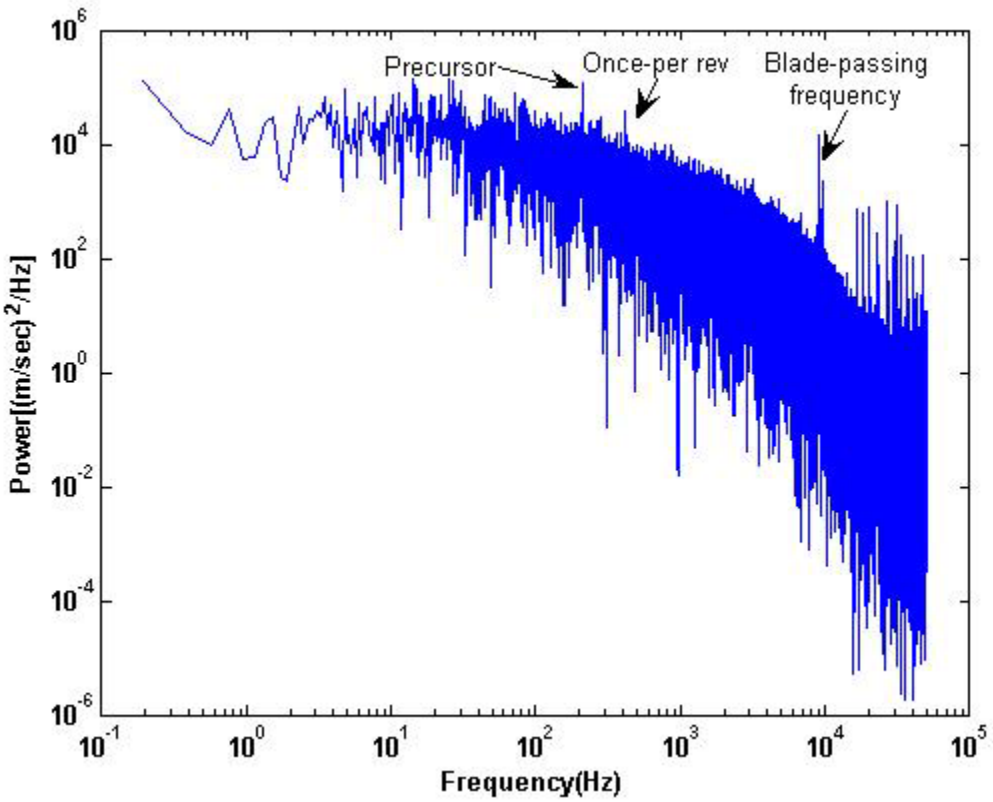

Figure 21. Power spectrum of hot-film data at 90 percent speed near stall

An autocorrelation was conducted on the data taken at 90 percent speed at a mass flow rate between peak efficiency and stall. A plot of the autocorrelation is shown in Figure 22, which shows an overall exponential drop off of the signal with time. This too is typical of free stream turbulence. The high frequency oscillation superimposed on the exponential decay is once again the blade-passing frequency. The area under the curve is an indication of the size of the length scale of the inlet turbulence.

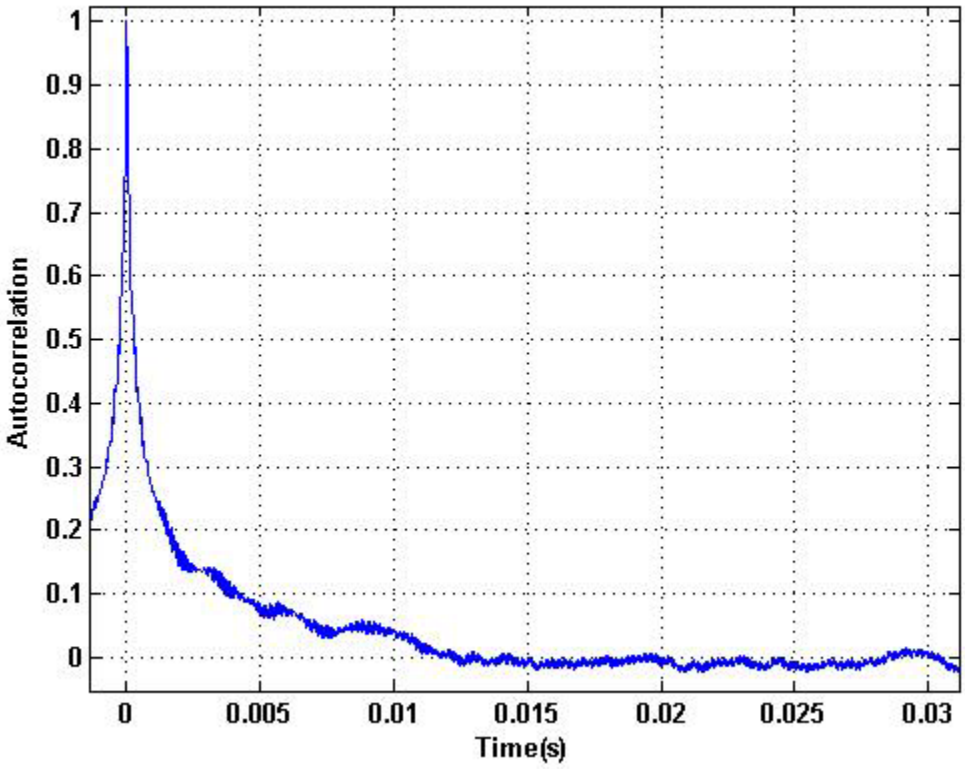

Figure 22. Autocorrelation of hot-film data at 90 percent speed between stall and peak efficiency

The autocorrelation conducted on the hot-film anemometry data taken near stall at 90 percent speed is shown in Figure 22. Besides the same overall trend as in Figure 21, a low frequency oscillation is apparent. This oscillation corresponded to a frequency of 200Hz which was about 50 percent of the rotor speed. This was convincing evidence of the presence of a modal stall precursor oscillation. Previous measurements by Gannon et al. (Ref 5), showed that the subsequent stall cell rotated at 60 percent of the rotor speed.

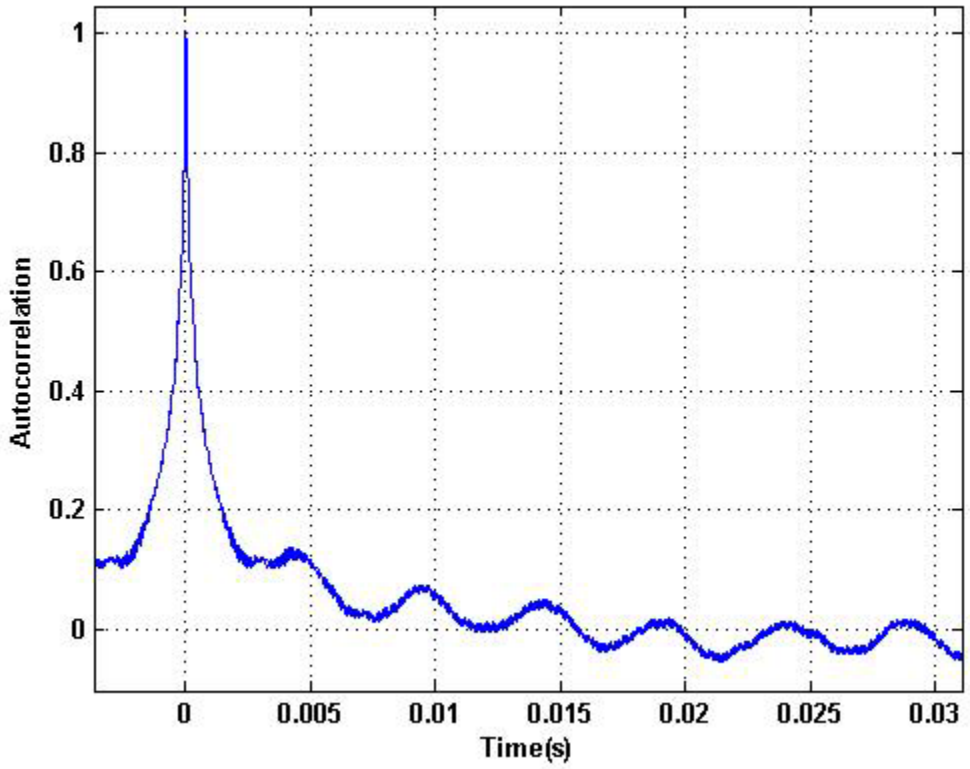

Figure 23. Autocorrelation of hot-film data at 90 percent speed near stall

The precursor oscillation was also found in the Kulite data near stall. A fast Fourier transform of Kulite data was used to create a contour plot of the power spectrum over time. Figure 24 shows data taken at peak efficiency. While the once-per-rev and blade-passing frequencies (or log thereof) were evident, the precursor frequency was not evident.

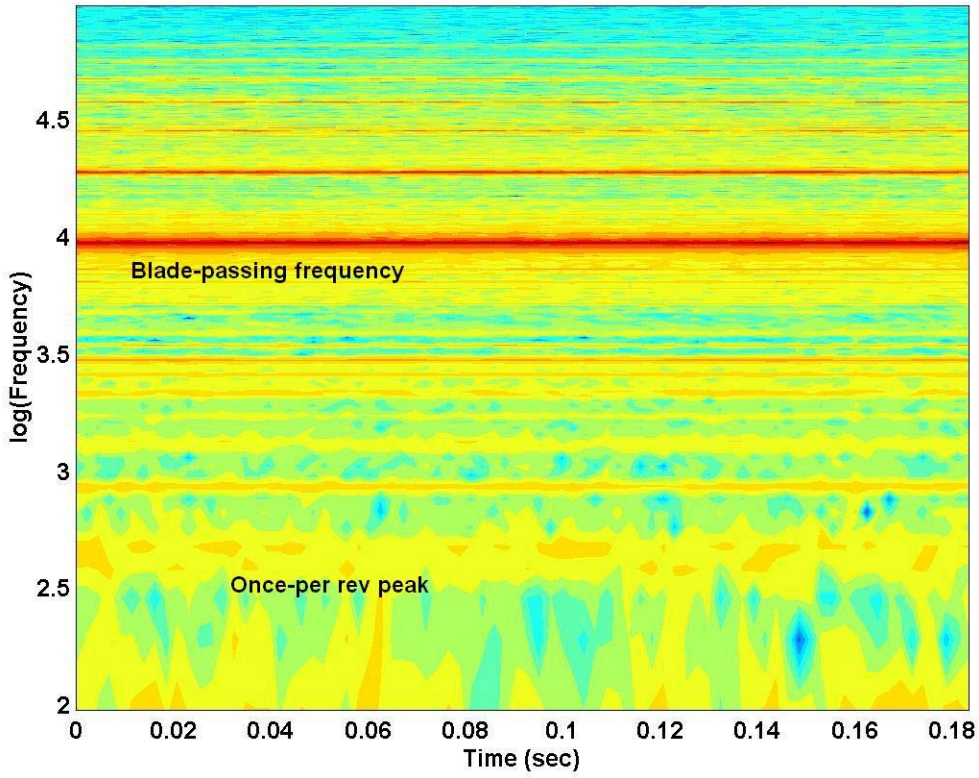

Figure 24. Power spectrum contour plot of Kulite data at 90 percent speed at peak efficiency

Figure 25 represents data taken near stall at 90 percent speed. The precursor oscillation, once per revolution, and the blade-passing frequency, can be seen in this contour plot.

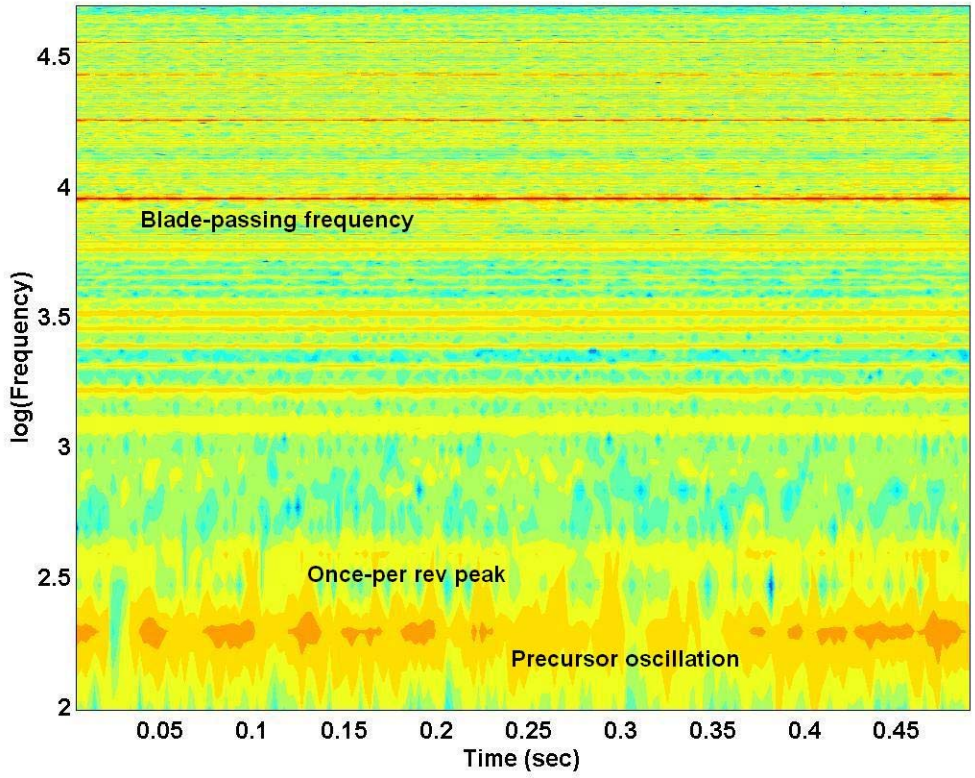

Figure 25. Power spectrum contour plot of Kulite data at 90 percent speed near stall

Figure 26 is a contour plot of Kulite data taken at 95 percent speed and close to stall. These data were taken at a mass flow rate that was not as close to the stall margin as the data represented in Figure 25, but precursor oscillation was also observed. Hot-film data at 95 percent speed are given in Appendix D. The measurement duration for these data samples was too short and yielded inconclusive frequency domain results.

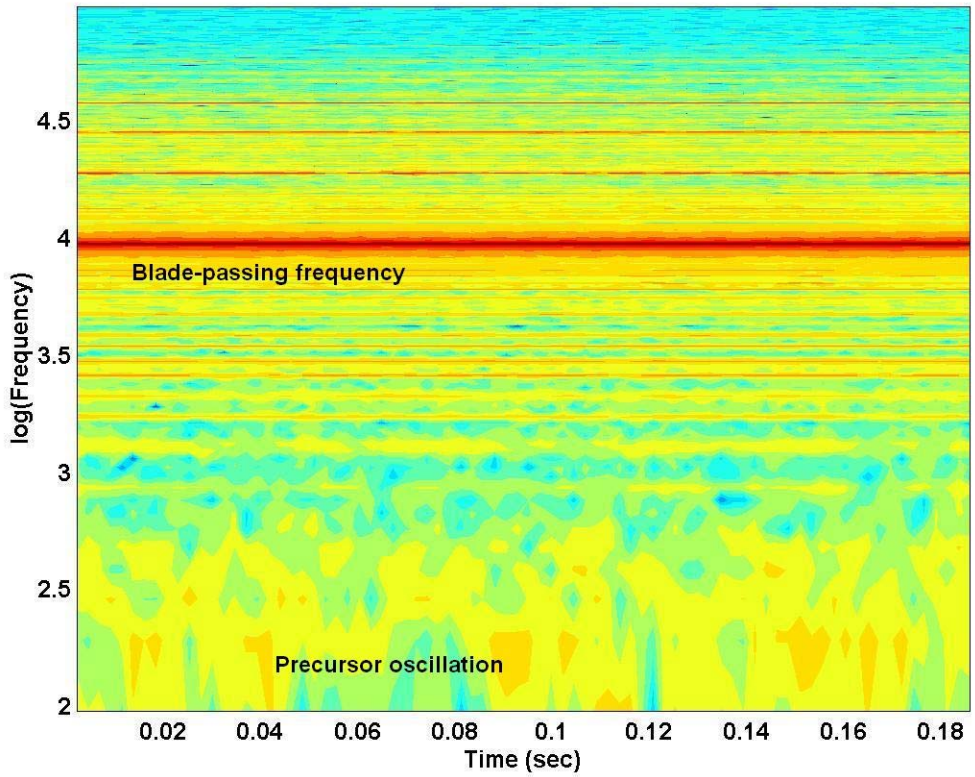

Figure 26. Power spectrum contour plot of Kulite data at 95 percent speed near stall

D. STEAM-INDUCED STALL AT 70% SPEED

Initial testing of steam-induced stall was conducted at 90 percent speed with the steam pipe connected directly to the inlet duct that connected the settling chamber to the test compressor. This method yielded unsatisfactory results due to the fact that the steam was bypassing the throttle and increasing the mass flow rate through the compressor. The additional mass flow prevented stall rather than inducing stall in the compressor rotor. This method was abandoned when it was discovered that stall was easily achieved by venting steam outside and allowing it to be ingested through the throttle. The mass flow rate of the steam ingested during this initial attempt was not measured but the data from the steam-induced stall are presented in Appendix C.

Figure 27 shows the hot–film, raw-voltage signal recorded by the high speed data acquisition system from the IFA 100, going into steam-induced stall at 70 percent speed.

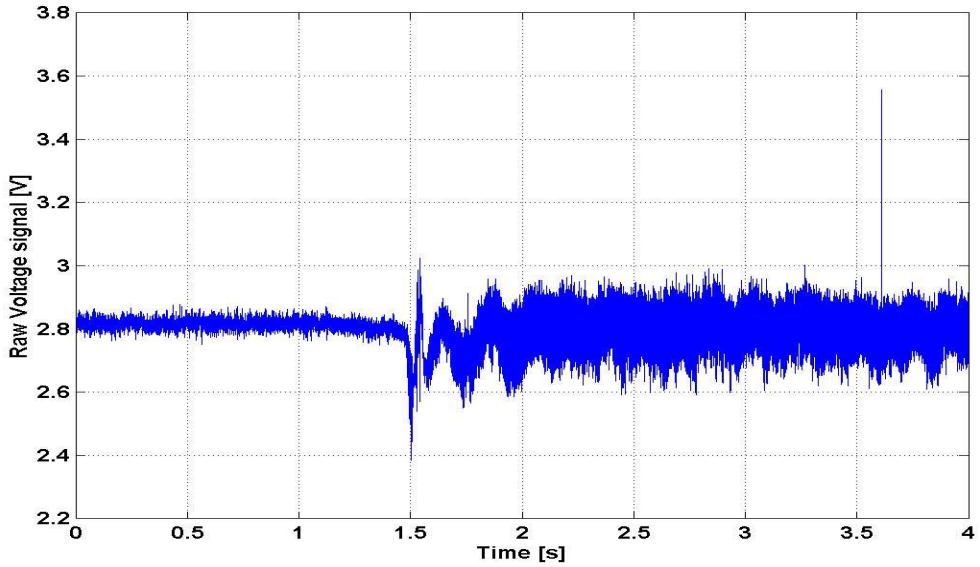

Figure 27. Raw-voltage hot-film signal going into steam-induced stall at 70 percent speed

Figure 28 is the raw-voltage of the Kulite signal going into steam-induced stall at 70 percent speed. Because both the Kulite and hot-film data were received by the VXI mainframe, the times scales on Figures 27 and 28 are identical.

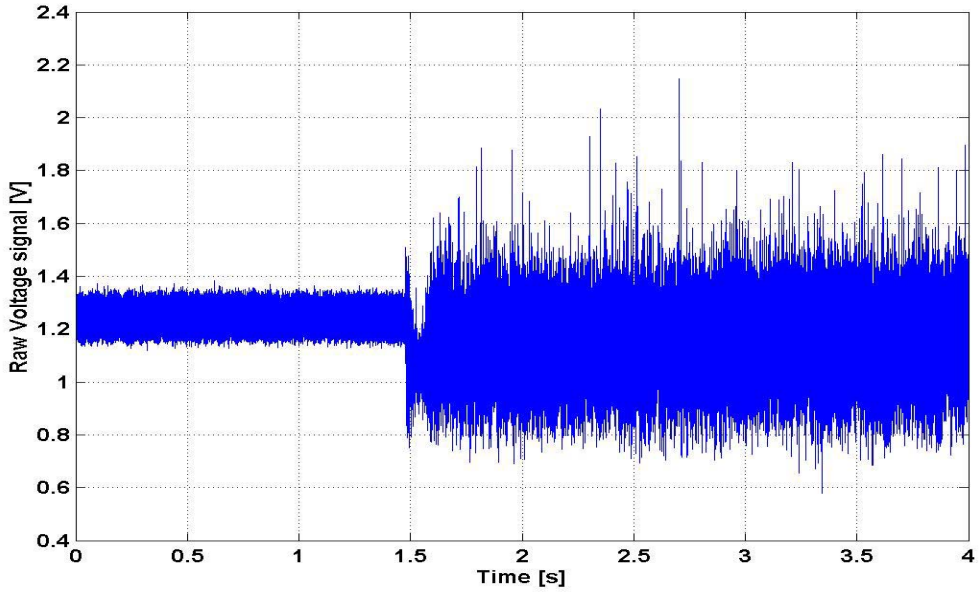

Figure 28. Raw-voltage Kulite signal going into steam induced stall at 70 percent speed

A fast Fourier transform was used to create a power spectrum of the hot-film data as seen in Figure 29. Blade-passing frequency, once per revolution frequency and the rotating stall cell frequency were all identifiable from this trace. The corresponding raw signal of these data is given in Appendix E.

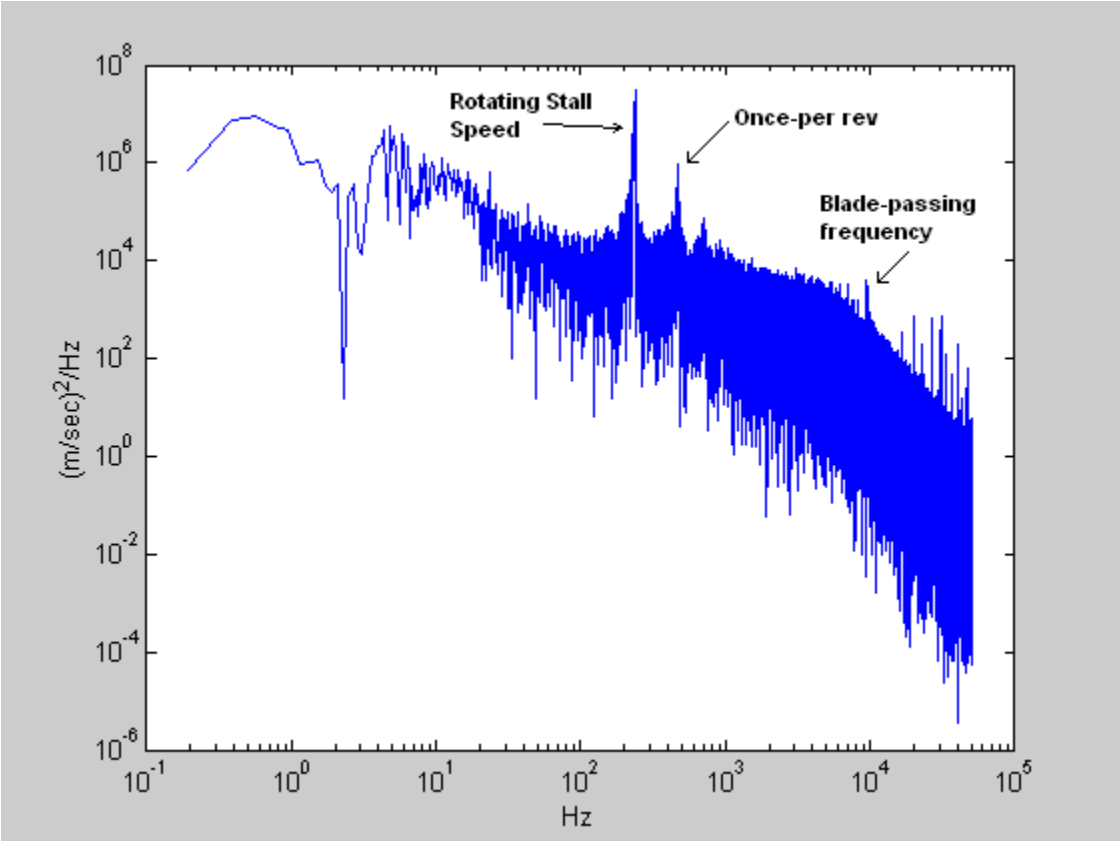

Figure 29. Power spectrum of hot-film data during steam-induced stall at 70 percent speed

The fast Fourier transform of the hot-film data was then evaluated over time to create a waterfall plot as seen in Figure 30. Figure 31 is the equivalent waterfall plot created from the Kulite data on the same time scale as the hot-film waterfall plot.

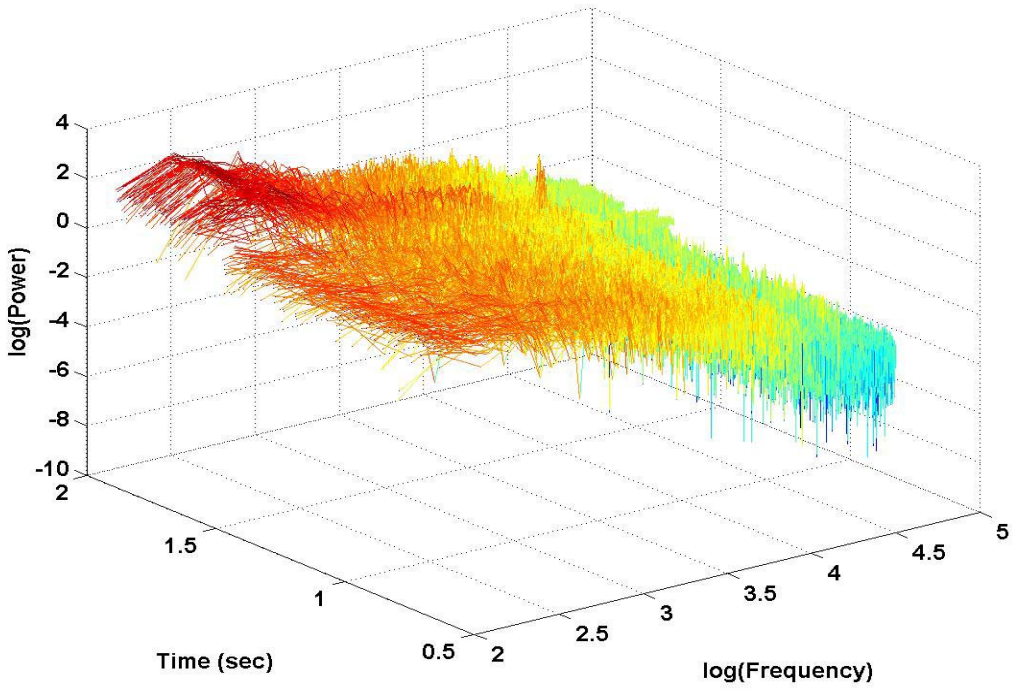

Figure 30. Waterfall plot of hot-film data going into steam-induced stall at 70 percent speed

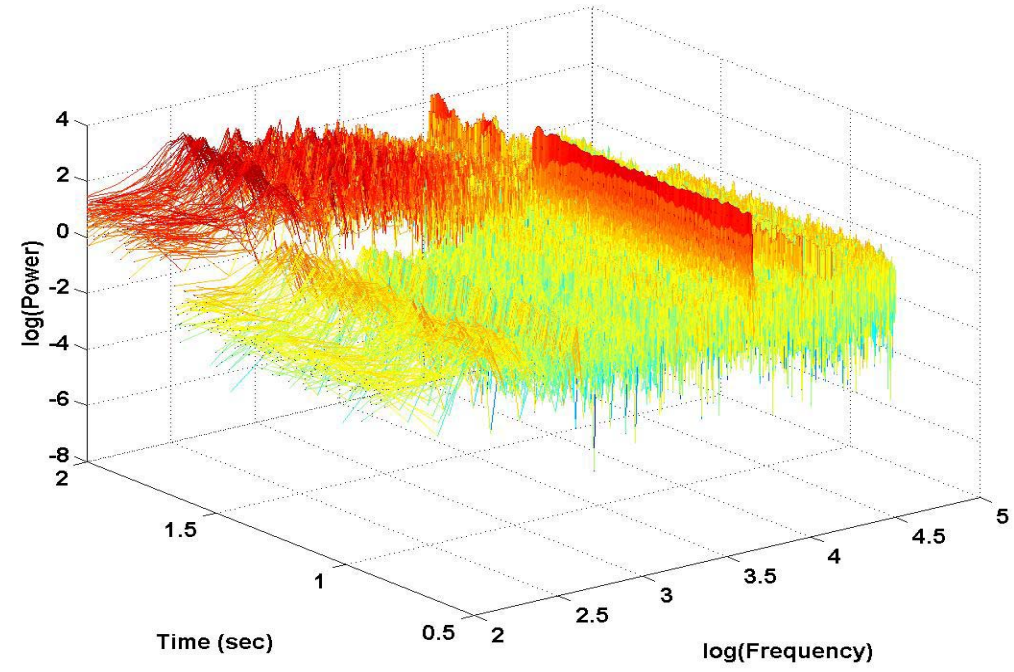

Figure 31. Waterfall plot of Kulite data going into steam induced stall at 70 percent speed

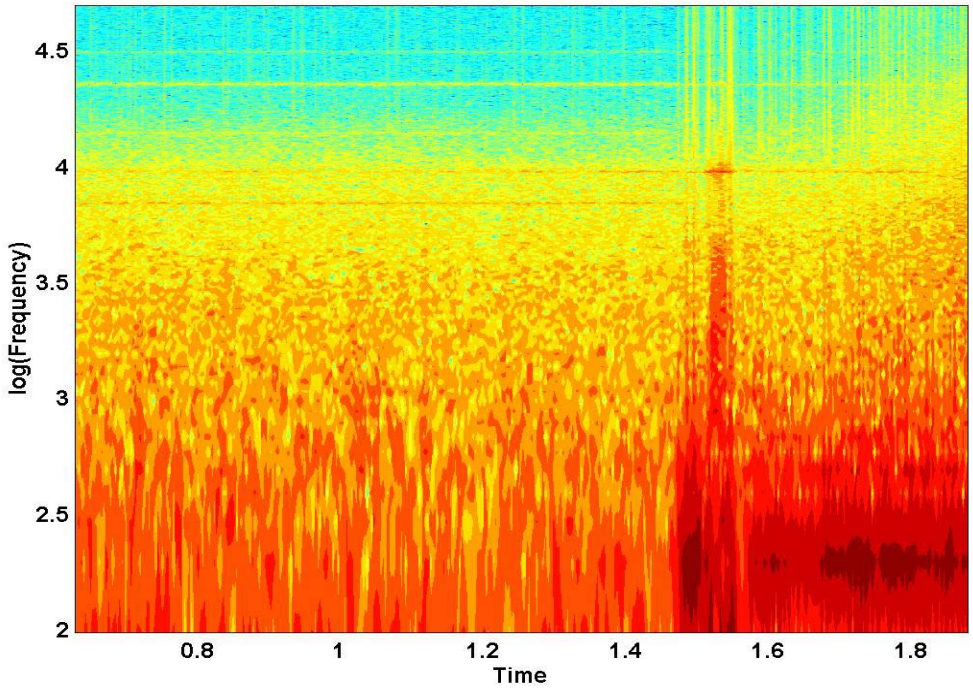

Figure 32. Contour plot of hot-film data going into steam-induced stall at 70 percent speed

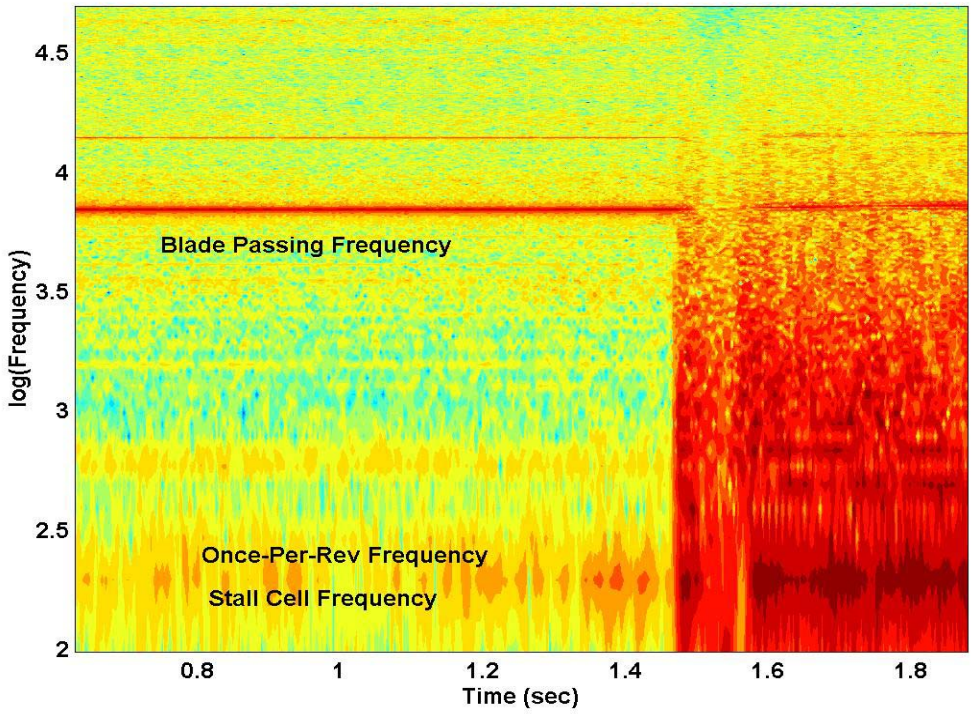

Figure 33. Contour plot of Kulite data going into steam-induced stall at 70 percent speed

Contour plots were also created from the fast Fourier transform. Figure 32 and 33 show the hot-film and Kulite data respectively.

The change in speed of the compressor going into steam-induced stall is shown in Figure 34.

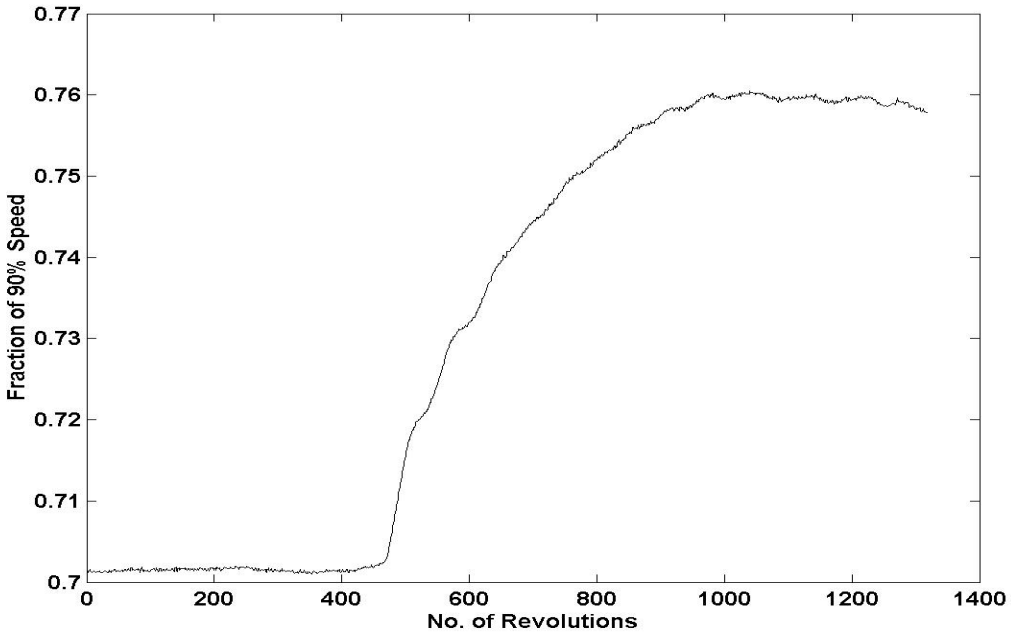

Figure 34. Change in compressor speed during steam-induced stall

The transient pressure measured in the steam line was used to calculate the mass flow rate of the ingested steam. Figure 35 shows the pressure change in the steam pipe as well as the temperature change in the inlet of the compressor over time during the steam-induced stall experiment. A pressure of 475 kPa was reached in the steam pipe prior to releasing steam into the compressor. By evaluating the change in pressure with respect to time during the first second, a steam mass flow rate of 0.06 kg/sec into the compressor was calculated.

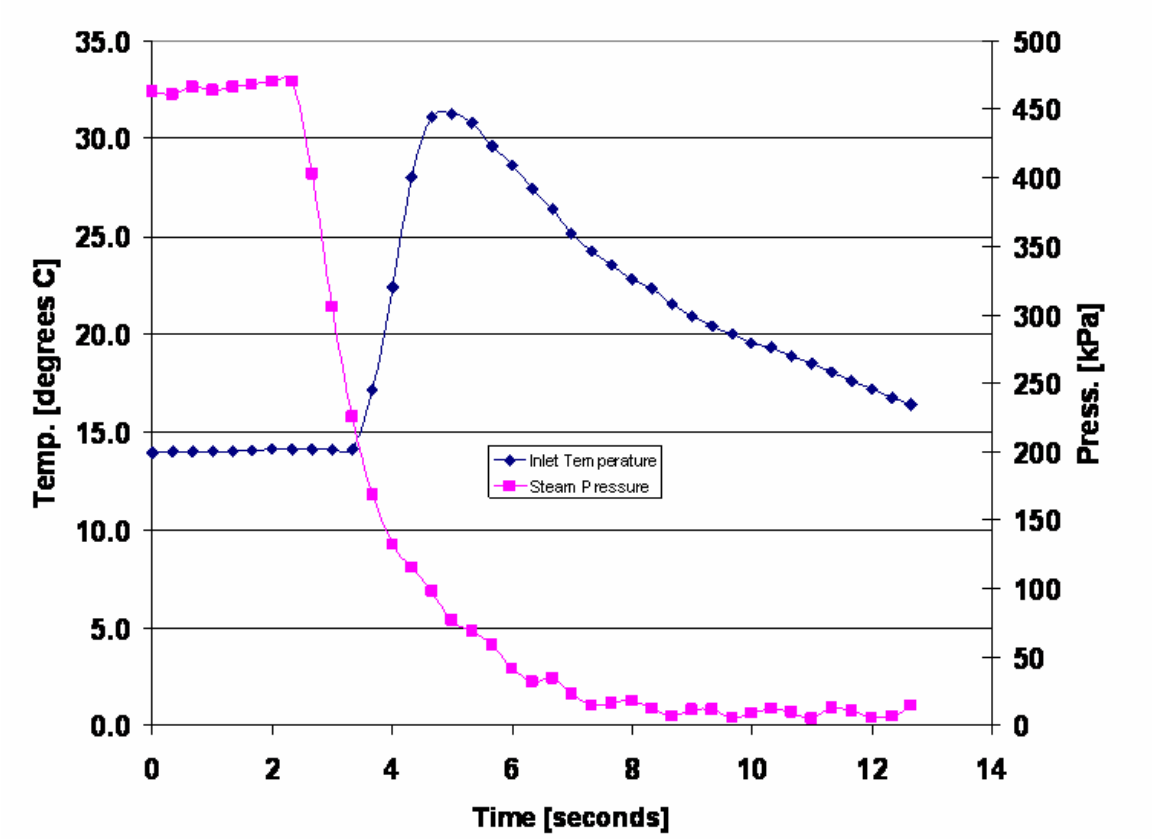

Figure 35. Steam pressure and inlet temperature change during steam-induced stall at 70 percent speed

A steam-induced stall of the rotor was observed at 70 percent speed at a mass flow rate of 4.30 kg/sec. Stall was not observed at higher mass flow rates using the given amount of steam. Transient data taken during steam ingestion but at a higher mass flow-rate which did not induce stall are given in Appendix F. Figure 36 shows the compressor map with the single point at 70 percent speed near stall that was measured prior to the steam ingestion experiment. At that point the compressor rotor stalled, hence the reduction in stall margin defined as $\left|\left(\dot{m}_{peak\_c0} - \dot{m}_{stall}\right)/\dot{m}_{peak\_c0}\right|$ was calculated to be from 0.30 to 0.25, i.e. a 17 percent reduction in stall margin

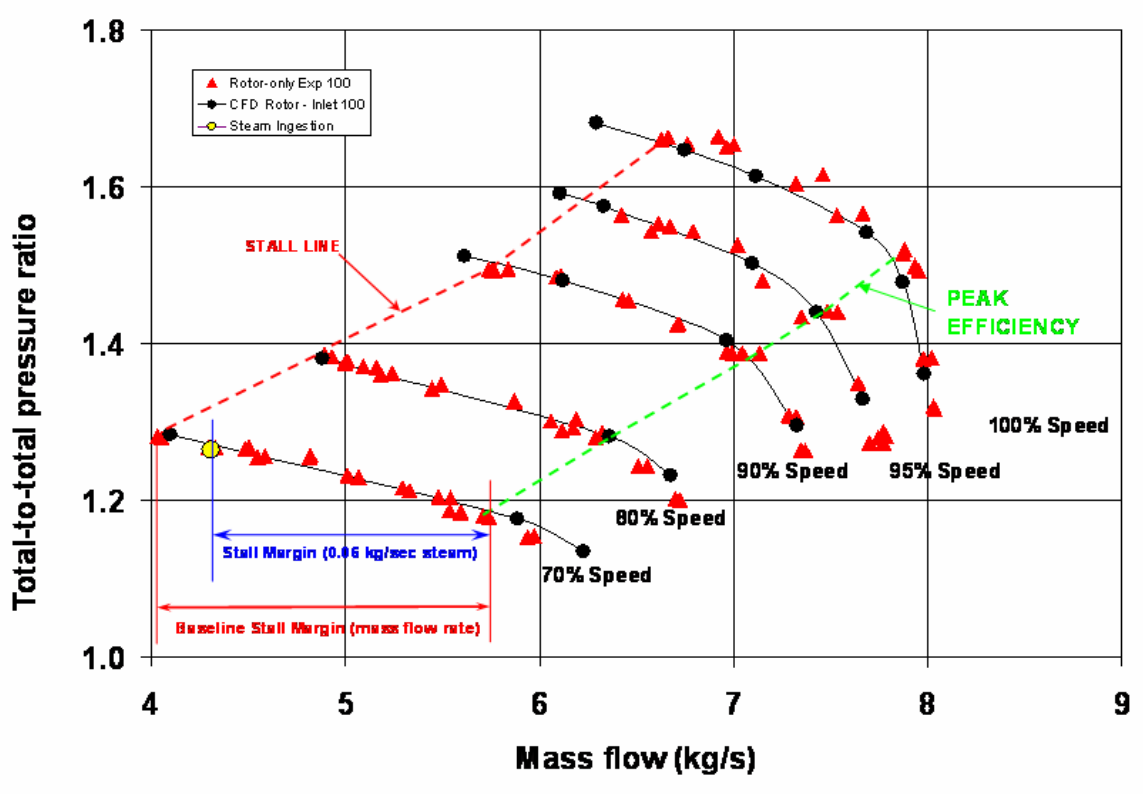

Figure 36. Compressor map with 70 percent speed steam-induced stall margin

THIS PAGE INTENTIONALLY LEFT BLANK

VI. CONCLUSIONS

Hot-film measurements were successfully conducted for the first time in the inlet to the transonic compressor rig over the rotor speed range of 70 to 95 percent of design speed. An average turbulence intensity of 2.26 percent with a variance of 0.287 was determined in the inlet flow of the compressor. Although variations in the turbulence intensity were observed, these variations were small and did not show a correlation with mass flow rate nor speed.

Performance measurements were carried out at 94 percent speed from open throttle to near stall. These data were taken to establish a speed line closer to 100 percent speed typical of an engine at cruise condition. These data follow those previously taken with respect to the trend of the total pressure ratio, and the value of the measured peak efficiency.

A precursor to stall oscillation was observed in the hot-film anemometry data as well as Kulite pressure transducer data. The precursor oscillation appeared to be at about half the rotor speed, and was only observable when the compressor was near stall.

The rotor was successfully stalled at 70 percent speed as a result of steam ingestion. The release of steam was controlled and the mass flow was determined. Synchronized transient data, from the hot-film probe and Kulite pressure transducer, were recorded prior to and during the steam-induced stall event. Stall was not observed at higher mass flow rates using the given amount of steam and therefore the effect of the steam on the stall margin was determined.

THIS PAGE INTENTIONALLY LEFT BLANK

LIST OF REFERENCES

1. Sanger, N.L. "Design of a Low Aspect Ratio Transonic Compressor Stage Using CFD Techniques", ASME Journal of Turbomachinery, Vol 118, pp.479-491, July 1996
2. Sanger, N. L., "Design Methodology for the NPS Transonic Compressor," TPL Technical Note 99-01, August 1999
3. Gannon, A.J., Hobson, G.V. and Shreeve ,R.P., 2004, "A Transonic Compressor Stage Part 1: Experimental Results, "ASME GT2004-53923, Turbo Expo, Vienna Austria.
4. Gannon, A.J., Hobson, G.V. and Shreeve ,R.P., "Measurement of the Unsteady Casewall Pressures Over a Rotor of a Transonic Fan and Comparison with Numerical Predictions", ISABE 2005, 17th International Symposium on Airbreathing Engines, Munich, September 2005.
5. Gannon, A.J., Hobson, G.V., Shreeve ,R.P., and Villescas, I.J., 2006, "Experimental Investigation During Stall and Surge in a Transonic Fan Stage & Rotor-Only Configuration", ASME GT2006-90925, Turbo Expo, Barcelona, Spain
6. Rodgers, M. W. Unsteady Pressure Measurements on the Case Wall of a Transonic Compressor, Master's Thesis, Naval Postgraduate School, Monterey, California, June 2003
7. Villescas, I., Flow Field Surveys In a Transonic Compressor Prior To Inlet Steam Ingestion Tests, Master's Thesis, Naval Postgraduate School, Monterey, California, September 2005
8. Brunner, M.D., Experimental and Computational Investigation of Flow in a Transonic Compressor Inlet, Master's Thesis, Naval Postgraduate School, Monterey, California, September 2005

9. O'Brien, J.M., Transonic Compressor Test Rig Rebuild and Initial Results with the Sanger Stage, Master's Thesis, Naval Postgraduate School, Monterey, California, June 2000.

10. Papamarkos, I., Inlet Distortion Generation for a Transonic Compressor, Master's Thesis, Naval Postgraduate School, Monterey, California, September 2004

11. Sussman Automatic Corporation. "SVS6 Electric Steam Boiler Specifications.", 2004, Long Island City, New York.

12. TSI Incorporated, http//www.tsi.com, 500 Cardigan Road, Shoreview, MN 55126

13. Brown, P. J., Experimental Investigation of Vortex Shedding in Flow Over Second-Generation, Controlled-Diffusion, Compressor Blades in Cascade, Master's Thesis, Naval Post Graduate School, Monterey, California, March 2002

14. MATLAB (version 5.3.0 R11), January 1999

APPENDIX A: HOT-FILM ANEMOMETRY CALIBRATION PROCEDURE

IFA 100 Setup

1. Record current temperature (Ta) and pressure (Pa).
2. Insert shorting probe and measure cable resistance (Rc).
    a. Pres [RES MEAS]
    b. Zero with [OPERATE RES] control knob
    c. Pres [RES MEAS]
    d. Record *Rc* then press [ENTER]
3. Replace shorting probe with hot wire probe
4. Repeat step #2 but DO NOT PRESS ENTER
5. Press [OPERATE RES] and adjust to operating resistance on box.
6. Press [BRIDGE COMP] and set with [BRIDGE] control knob according to the following table:

Sensor Type	Standard 1
T1.5	35
-P2	83
-PI1.5	115
-PI5	120
Metal Clad	775
-10A	70
-10	70
-20	115
-60	250

7. Press [RUN]
8. Start wind tunnel
9. Turn [CABLE COMP] knob counterclockwise until OSC light comes on then turn clockwise until it goes off plus another half turn.
    note: it is recommended that step 9 be performed with the wind tunnel velocity closer to the upper bound of expected experimental velocity.
10. The Low Flow Voltage (Eo) and High Flow Voltage (Em) need to be acquired in order to calculate GAIN and OFFSET. Eo and Em are the lower and upper bounds of the velocities expected during the experiment. Run the tunnel at both of these velocities and record the voltages.
11. On the IFA main screen select [CALIBRATION] then select [PROBE DATA]
    a. Select [OPEN CAL FILE]. This creates a calibration file. It is recommended that this file be named after serial number of probe.
    b. Select [GAIN & OFFSET]
    c. Enter the voltages recorded in step 10 in the high flow and low flow box.
    d. Select [CALCULATE] and record gain and offset values.

12. In the CAL METHOD block, select option 2, “Acquire E and Type dP.”
13. Select [CALIBRATE]
14. Enter current conditions on the left hand side of the screen remembering to select an appropriate dP unit. The dP is the difference between static and stagnation pressure and is used by the software to calculate the average velocity for each calibration point.
15. On the right hand side of the screen, enter the number of calibration points that will be taken.
16. For each calibration point, enter dP and reading and then press enter or click mouse outside of dP box. The IFA software should have calculated a velocity the dP reading. Press [Acquire] to record calibration point.
17. After all calibration points have been taken, close graph and press [Next Screen].
18. Select [Curves].
19. At bottom of screen, in the “fit” block, select King’s law. Record King’s law coefficients in calibration sheet for future data analysis.

Hot Wire Probe Calibration Data Sheet

Probe Serial Number	Model Number	Channel
70536123	**1212-20**	**1**

Date: _13_/OCT__/_05_

Ta Ambient Temp	Pa Atm Pressure	Rc Cable Resistance	Ro Res. w/ probe	Rop Oper. Res	Bridge	Eo L Flow	Em H Flow
14.8C	29.97"Hg	1.236	5.842	8.92	115	1.250	3.275

Gain	Span	Offset
2		2

	Delta P (kPa)	Velocity (m/s)	Voltage	RPM
1	0.846	37.796	2.624	8,000
2	1.369	48.027	2.810	11,000
3	2.212	60.885	2.935	13,570
4	3.305	74.164	3.050	16,350
5	4.304	84.369	3.138	19,045
6	5.168	92.201	3.185	21,040
7	6.743	104.807	3.252	24,450
8	7.654	111.352	3.275	26,875
9				
10				

Kings Law Coefficients

A= -26.45895	**B=23.24134**	**n=0.10000**

Hot Wire Probe Calibration Data Sheet

Probe Serial Number	Model Number	Channel

Date: _____/_____/_____

Ta Ambient Temp	Pa Atm Pressure	Rc Cable Resistance	Ro Res. w/ probe	Rop Oper. Res	Bridge	Eo L Flow	Em H Flow

Gain	Span	Offset

	kPa	Velocity	Voltage	
1				
2				
3				
4				
5				
6				
7				
8				
9				
10				

Kings Law Coefficients

A=	B=	n=

APPENDIX B: MATLAB M-FILES

The following file was used to calculate the average velocity and turbulence intensity as well as plot the Fast Fourier Transform of the data.

```
function [turbint,avevel]=hotwirefft(king,file)

% This function will calculate the average velocity,
% turbulance intensity, and the Fast Fourier Transform.
% format for file is '03NOV5.E0005'
% kings law coeff must be in a matrix with probes as rows. (a b n)
% for example k=[.87726 .31691 .52]
close all

a=dlmread(file);
b=dlmread(file);

%This program is writen for sample size of 4096

    for n=1:4096
        a(n,3)=(((a(n,2)*a(n,2))-king(1,1))/(king(1,2)))^(1/king(1,3));
    end
    avevel_1=mean(a(:,3))
    sd_1=std(a(:,3));
    turbint_1=(sd_1*100)/avevel_1

    Figure(1)
    plot(a(:,1),a(:,3))
    xlabel('sec')
    ylabel('m/sec')

%the following performs the Fast Fourier Transform
    voltage=b(:,2);
    N=length(voltage)-1;
    deltat=.00001;

    Y = fft(voltage);
    Y(1)=[];
    n=length(Y);
    power = abs(Y(1:n/2)).^2;
    nyquist = .5;
```

```
freq = (1:N/2)/(N*deltat);

Figure(2)
loglog(freq,power)
xlabel('Hz')
ylabel('(m/sec)^2/Hz')
```

The following file was used to plot the Fast Fourier Transform and Auto Correlation of the data.

auto_fft.m

```
close all
clear all

a=dlmread('23NOV05.E0006');
time=a(:,1);
voltage=a(:,2);

%This will plot the raw voltage trace
Figure(1)
plot(time,voltage)
xlabel('time')
ylabel('voltage')
title('Raw Signal')

N=length(voltage)-1;
deltat=.00001;

Y = fft(voltage);
Y(1)=[];
n=length(Y);
power = abs(Y(1:n/2)).^2;
nyquist = .5;
freq = (1:N/2)/(N*deltat);
Figure(2)
loglog(freq,power)
xlabel('freq')
ylabel('power')
title('Periodogram')

% this will plot the auto correlation of the data
```

```
Figure(3)
auto_time=deltat*lags;
plot(auto_time,C)
grid on
```

Find Loc

```
% Find_loc
% m-function file to find the position of the trigger for each    % once per rev

function [Loc] = Find_loc(time,tach);

% Number of samples
samples = length(time);

% Trigger level is calculated
Trig = mean([min(tach) max(tach)]);

% Location of trigger points and correction to exact trigger
% timing point
Loc = find( tach(2:samples)<Trig & tach(1:samples-1)>Trig );
% Location of time of start of rev
```

Mov_ave.m

```
% m-function file to calculate the moving averages at a
% particular point
% x,y data
% points ahead and behind central one ie 0 return same data, 1 =
% 3 points, 2 = 5 points
% n, polynomial to fit, 0 = average, 1 = linear, 2 = parabolic
% etc

function [y_avg] = mov_avg(x,y,points,N)

y_avg = y;

x_poly = zeros(1,(2*points+1));
y_poly = zeros(1,(2*points+1));

for i = (points+1):((length(x)-points)-1)
    for j = -points:points
```

```
            x_poly(j+points+1) = x(i+j);
            y_poly(j+points+1) = y(i+j);
        end
        y_avg(i) = mean([max(y_poly) min(y_poly)]); % Most effective method, just take
the mean of the max and min
    end

    % Leading points
    if points > 0
        % Leading few points
        for j = 1:(2*points+1)
            y_poly(j) = y(j);
        end

        % Leading moving average
        for i = 1:points
            y_avg(i)  = mean([max(y_poly) min(y_poly)]);
        end
    % for i = 1:points

        % Trailing few points
        for j = (2*points+1):-1:1
            y_poly(j) = y(length(x)-j+1);
        end

        % Trailing moving average
        for i = (length(x)-points):length(x)
            y_avg(i)  = mean([max(y_poly) min(y_poly)]);
        end % for i = 1:points
    end % if points > 0
```

plot_data.m

```
% m-file to plot a certain time part of the stall data file

function [fred] = Plot_data(fig_no,Raw_data)

% Time period is defined
time_start = Raw_data(1,1);   % Start time of sample
time_end   = Raw_data(end,1); % End time of sample
%time_start = 16.3            % User defined start time
%time_end   = 17              % User defined end time

% Time period entry points are found
```

```
temp = find(Raw_data(:,1)>time_start & Raw_data(:,1)<time_end);

% Figure is plotted and trimmed
%if bool_new_fig
    Figure(fig_no); close; Figure(fig_no);
    %else
    %Figure(fig_no);
    %end

%if subplot_no ~= 0
%    subplot(subplot_tot,1,subplot_no)
%end % if subplot_no ~= 0

plot(Raw_data(temp,1),Raw_data(temp,3),'b')
%hold on
xlabel('Time [s]'); ylabel('Raw Voltage signal [V]')
grid on

temp = axis;
%h = line([time(Loc(1:end),Data_column)
time(Loc(1:end),Data_column)]',(ones(size(Loc(1:end)))*([temp(3) temp(4)]))');
%set(h,'Color',[0 0 0]);  % Makes colour of line black
%h = line([time(Loc(2:end),Data_column)-time_err time(Loc(2:end),Data_column)-
time_err]',(ones(size(Loc(2:end)))*([temp(3) temp(4)]))');
%set(h,'Color',[0 0 0]);  % Makes colour of line black

%axis([temp(1) temp(2) 0 0.7])

%if subplot_no ~= 0
%    axis([0 120 0.5 1.3])
%end % if subplot_no ~= 0
```

plot_data_HW.m

```
% m-file to plot a certain time part of the stall data file

function [fred] = Plot_data(fig_no,Raw_data)

% Time period is defined
time_start = Raw_data(1,1);   % Start time of sample
time_end   = Raw_data(end,1); % End time of sample
%time_start = 16.3            % User defined start time
%time_end   = 17              % User defined end time
```

```
% Time period entry points are found
temp = find(Raw_data(:,1)>time_start & Raw_data(:,1)<time_end);

% Figure is plotted and trimmed
%if bool_new_fig
    Figure(fig_no); close; Figure(fig_no);
    %else
    %Figure(fig_no);
    %end

%if subplot_no ~= 0
%    subplot(subplot_tot,1,subplot_no)
%end % if subplot_no ~= 0

plot(Raw_data(temp,1),Raw_data(temp,6),'b')
%hold on
xlabel('Time [s]'); ylabel('Raw Voltage signal [V]')
grid on

temp = axis;
%h = line([time(Loc(1:end),Data_column)
time(Loc(1:end),Data_column)]',(ones(size(Loc(1:end)))*([temp(3) temp(4)]))');
%set(h,'Color',[0 0 0]);  % Makes colour of line black
%h = line([time(Loc(2:end),Data_column)-time_err time(Loc(2:end),Data_column)-
time_err]',(ones(size(Loc(2:end)))*([temp(3) temp(4)]))');
%set(h,'Color',[0 0 0]);  % Makes colour of line black

%axis([temp(1) temp(2) 0 0.7])

%if subplot_no ~= 0
%    axis([0 120 0.5 1.3])
%end % if subplot_no ~= 0
```

Plot_rpm.m

```
% mfile to plot RPM through the stall

function [fred] = Plot_rpm(fig_no,RPM)

%temp = find(Raw_data(:,9)>0);

Figure(fig_no);% close; Figure(fig_no);
%plot(Raw_data(temp,1),Raw_data(temp,9))
%plot(RPM(:,1),RPM(:,2),'k');
```

```
plot(RPM(:,2),'k');
hold on
xlabel('No. of Revolutions'); ylabel('Fraction of 90% Speed'); title('RPM through stall at 90% speed')
```

Process_data.m

```
% m function file to organise the data of the Raw data file

function [time,volts,tach,Loc,RPM] = Process_data(Raw_data)

% Data is sorted into simpler to use groups
time    = Raw_data(:,1);    % Kulite time data
volts   = Raw_data(:,2:5); % Kulite raw voltage data
tach    = Raw_data(:,7);   % Kulite trigger voltage
samples = length(time);     % Number of samples

% Trigger level is calculated
Trig = mean([min(tach) max(tach)]);

% Location of trigger points and correction to exact trigger
% timing point
Loc = find( tach(2:samples)<Trig & tach(1:samples-1)>Trig ); %location of time of start of rev
Hz = (length(Loc)-1)/(time(Loc(end))-time(Loc(1)));
% Frequency of rotor revolution over the sample period

% If Loc (location) if at the beggining of the sample it is
% discarded
if Loc(1) < 3
    Loc = Loc(2:end);
end

% Last trigger is discarded to ensure trailing zeros resulting
% from probe lining up do not effect the calculations.
Loc = Loc(1:(end-1));

% Timing correction to ensure that each sample begins at the
% correct time
d_time_Loc(:,1) = time(Loc+1)-time(Loc);
% Time interval between trigger and next time interval
d_tach_Loc(:,1) = tach(Loc+1)-tach(Loc);
% Ramp slope between trigger and next time interval
```

```
m               = d_tach_Loc./d_time_Loc; % Slope
c               = tach(Loc);              % Intercept
time_err        = (Trig - c)./m;          % Error in trigger
                                                  % timing


% Error in trigger timing is converted to be directly subtracted
% from the period
% time_err = (time_err(2:end)-time_err(1:end-1));

% The RPM based on each trigger is calculated
RPM = time(Loc(2:end)) - time(Loc(1:end-1));
RPM = RPM + (time_err(2:end)-time_err(1:end-1));
RPM = 60./RPM;

%Hz_old = Hz;
RPM    = [time(Loc(2:end)) RPM];
% First column is time signal and the second is the RPM

% Data is moving averaged a few times to remove the wiggle
%for i = 1:N_mov_avg
%    [Hz(:,2)] = mov_avg(Hz(:,1),Hz(:,2),1,1);
%end % for i = 1:,N_mov_avg
%[Hz(:,2)] = mov_avg(Hz(:,1),Hz(:,2),1,1);
%[Hz(:,2)] = mov_avg(Hz(:,1),Hz(:,2),1,1);
%[Hz(:,2)] = mov_avg(Hz(:,1),Hz(:,2),1,1);

% This is to correct the RPM
%time_err = time_err + (Hz(:,2)-Hz_old);
%[1./Hz_old 1./Hz(:,2) 1./(time(Loc(2:end))-time(Loc(1:end-1))+time_err)]

% Data is converted to Hz or RPM
%Hz(:,2) = 1./Hz(:,2);
```

Stall_70.m

```
%Stall90

%M-file to pull in stall data and plot it out
% 70% speed at surge

close all;
clear all;
```

```
%Raw data
tic
Raw_data=dlmread('Dx2005_1123_0958_70_6_10.csv',',','A6..H400000');
toc
%tach=Raw_data(:,8);
%time=Raw_data(:,1);
data=Raw_data(:,2:6);

% Constants
RPM_design = 27085;         % Design RPM in RPM
RPM_Hz     = RPM_design/60; % Design RPM in Hz

[time,volts,tach,Loc,RPM] = Process_data(Raw_data);
[RPM(:,2)]                = mov_avg(RPM(:,1),RPM(:,2),1,1);

%Input value for number of revs
B=input('Enter a binary minus one (such as 511 for one rev) to select the number
of revs:');

timeshort1=time(1:B,1);
deltat1=(timeshort1(end,1)-timeshort1(1,1))/(length(timeshort1));
%deltat1=(timeshort1(end,1)-timeshort1(1,1))/(length(timeshort1)-1);
[Loc] = Find_loc(time,tach);
kulite1=data(:,1);

%_____________________________________________________________________________
_____________
%Figure 1;
%_A particular column of the data is plotted
plot_data(1,Raw_data);
title('Stage Surge 90%');

%_____________________________________________________________________________
_____________
%Figure 2;
%_The RPM is plotted
plot_rpm(2,RPM/RPM_design);
title('Stage Surge 90%');

%_____________________________________________________________________________
_____________
%Figure 3;
%The beginning of stall is graphed on a waterfall plot
%Figure(3);
```

```
count=1;
A1=200;
A2=600;
for A=A1:A2;

    %_Locates triggers
    LocA=(Loc(A):(Loc(A)+B));

    yfftA=kulite1(LocA,1);
    Ya=fft(yfftA);
    Ya(1)=[];
    power1=abs(Ya(1:(length(yfftA)/2))).^2;
    N1=length(yfftA);
    n1=(1:(N1)/2)';
    freq1=(n1)/((N1)*deltat1);

    time1=(time(Loc(A)))*(ones(size(freq1)));

    if 0
        hold on;
        Figure(A);
        semilogy(freq1,power1,'r');

    end

    freq_fall(count,:)=freq1';
    power_fall(count,:)=power1';
    time_fall(count,:)=time1';

    count=count+1;

end

power_fall=log10(power_fall);
freq_fall =log10(freq_fall);

%_Graphs a waterfall plot
%waterfall(freq_fall,time_fall,power_fall);

%_Graph settings
ylabel('log(Frequency)');
xlabel('Time');
zlabel('log(Power)');
```

```
%title('Stage Surge 70%: Entering Stall at Triggers 10-30');
grid on;

%_____________________________________________________________________________
_____________________

%Figure 4
%The beginning of stall is graphed on a contour plot
%Figure(4);
count=1;
%for A=A1:A2;
 %   contourf(time_fall,freq_fall,power_fall,15);
    shading flat

    %_Graph settings
    xlabel('Time');
    ylabel('log(Frequency)');
    %title('Stage Surge 70%: Entering Stall at Triggers 10-30');
    grid on;
    %axis([time(Loc(A1)) time(Loc(A2)) 2 5]);

    count=count+1;
    %end
```

THIS PAGE INTENTIONALLY LEFT BLANK

APPENDIX C: 90 PERCENT AND SPEED STEAM-INDUCED STALL: HOT-FILM AND PRESSURE DATA

Hot-film file 10NOV05.E0015

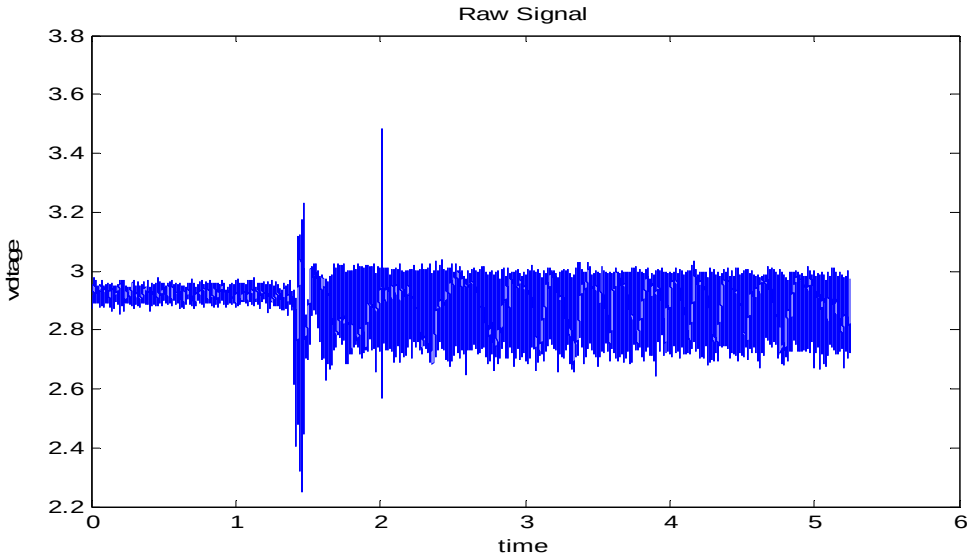

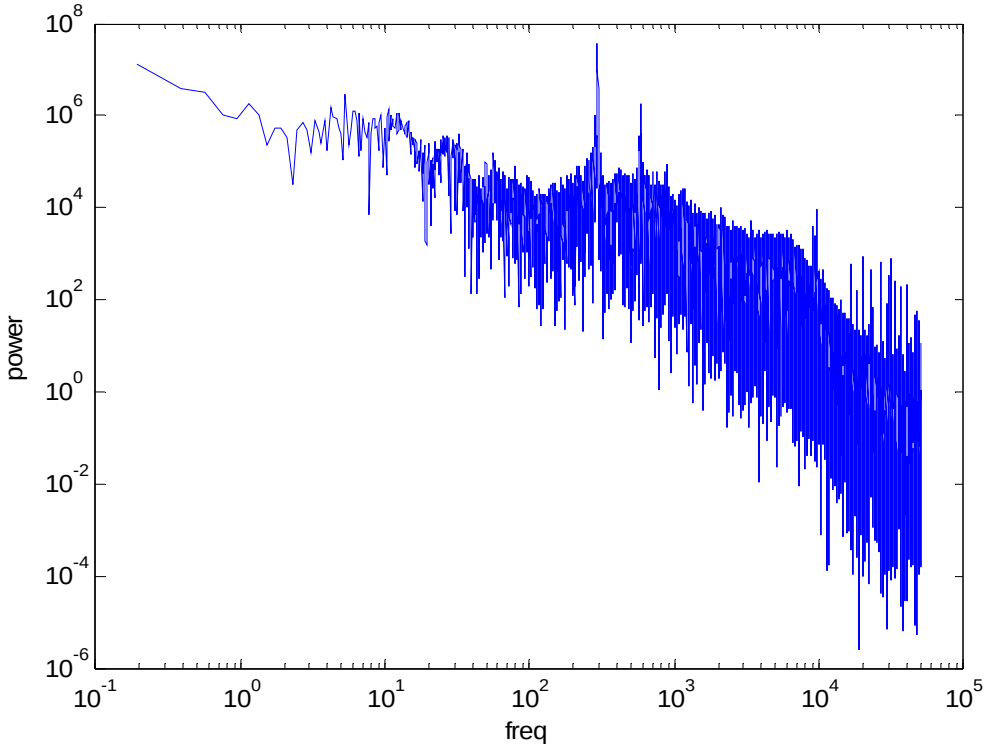

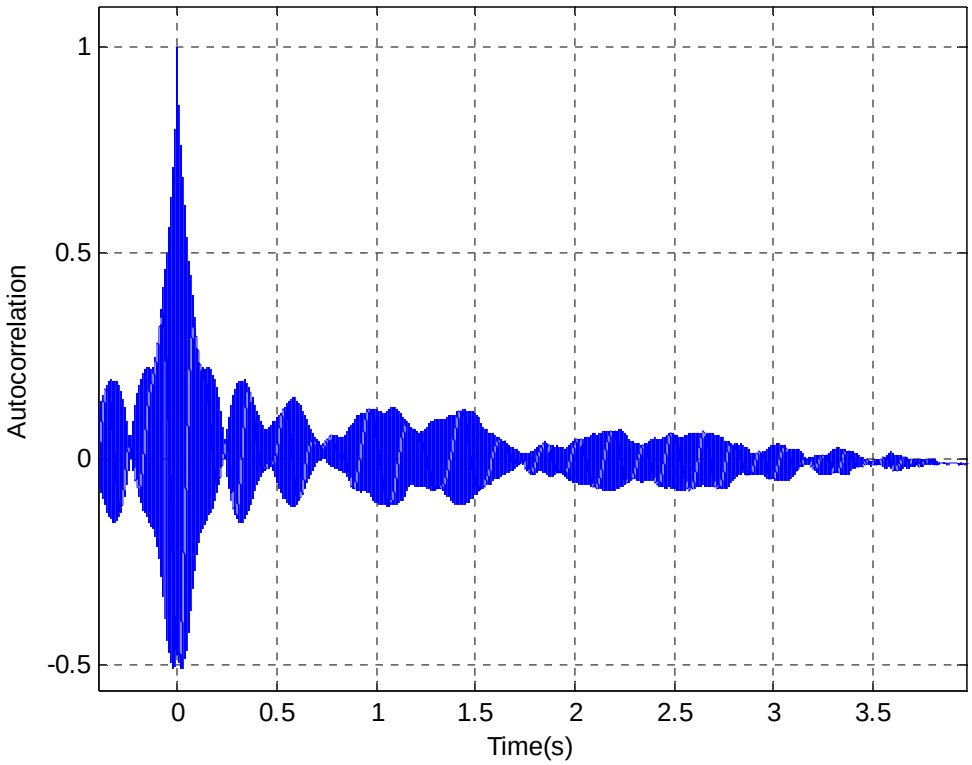
1
0.5
0
-0.5
Autocorrelation
0
0.5
1
1.5
2
2.5
3
3.5
Time(s)

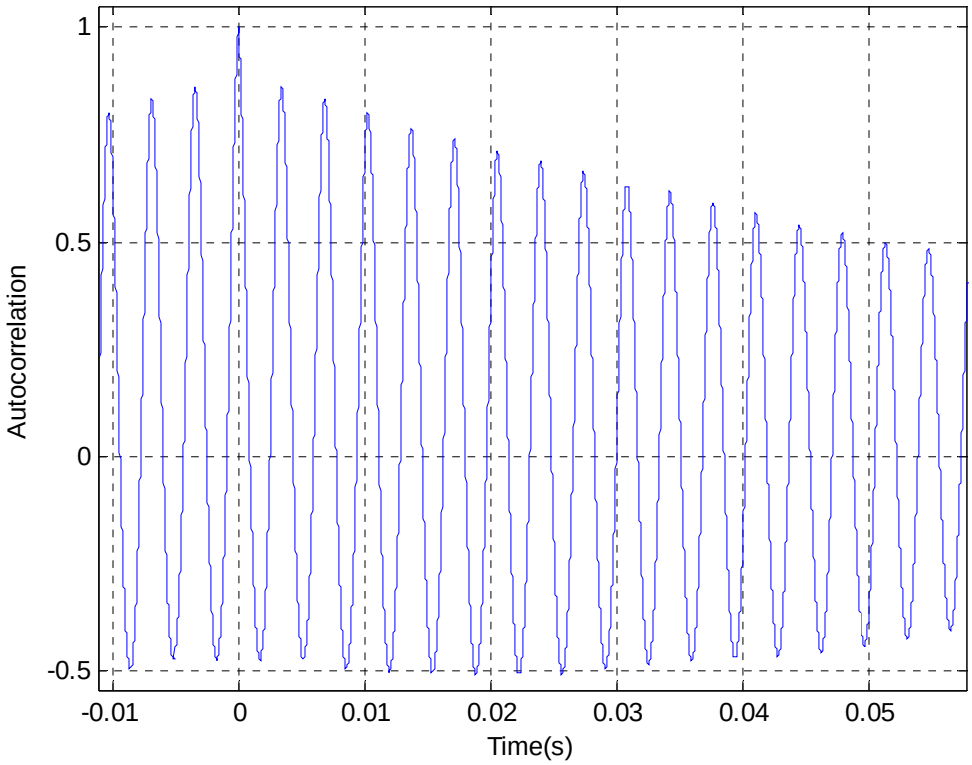
1
0.5
0
-0.5
Autocorrelation
-0.01
0
0.01
0.02
0.03
0.04
0.05
Time(s)

Waterfall plot of 10NOV05.E0015 hot-film data file

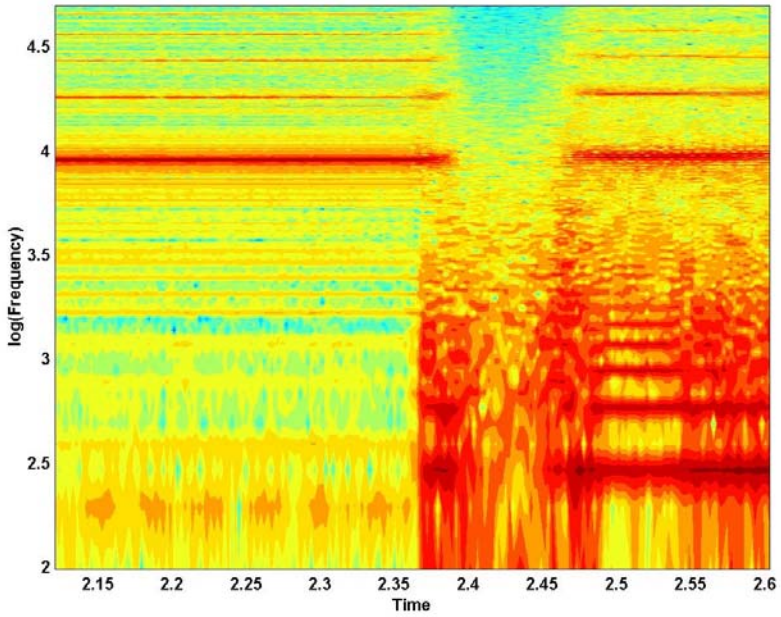

Waterfall plot of Kulite data.

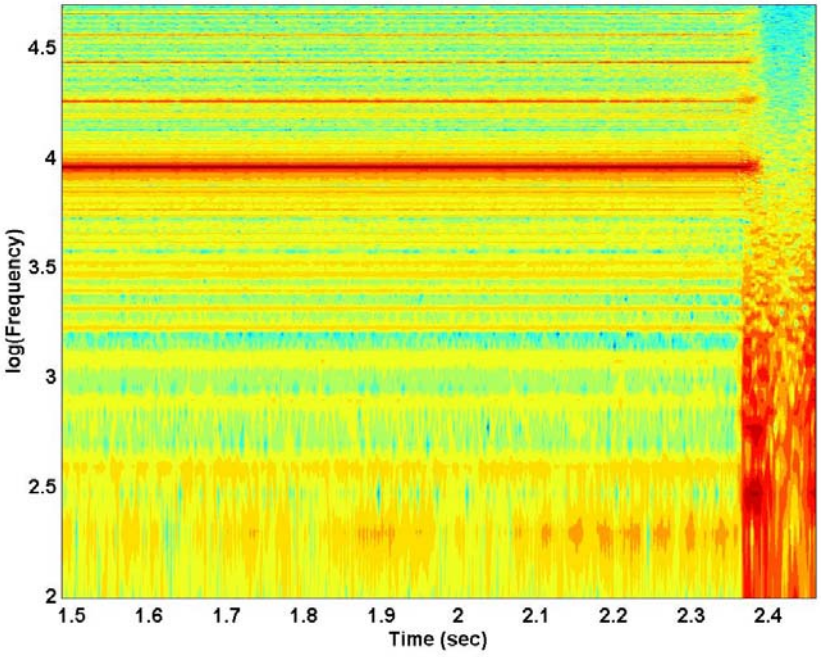

THIS PAGE INTENTIONALLY LEFT BLANK

APPENDIX D: 95 PERCENT SPEED NEAR STALL: HOT-FILM DATA

Data file 03NOV05.E0010

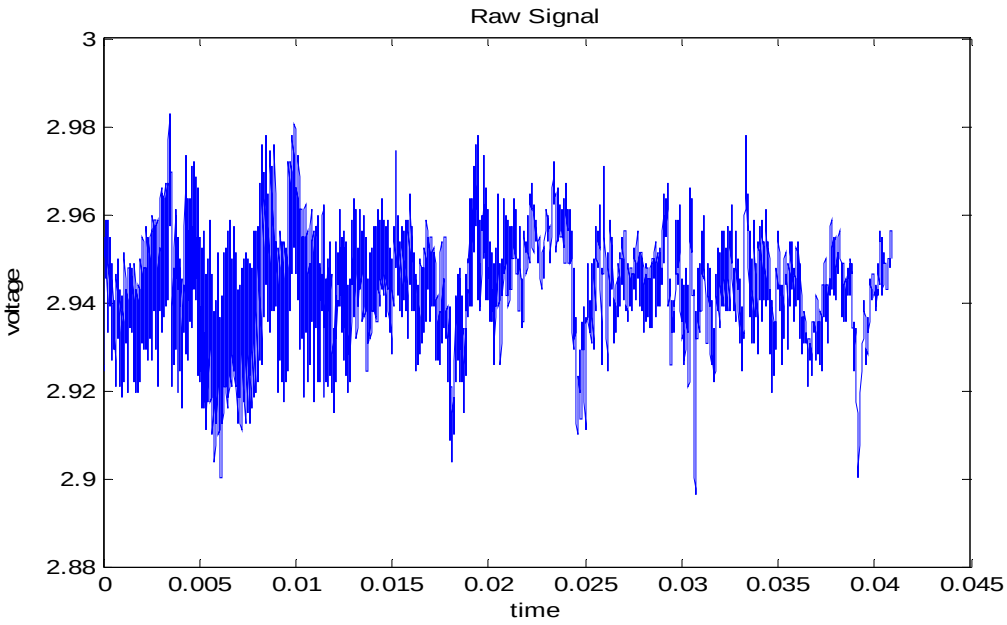

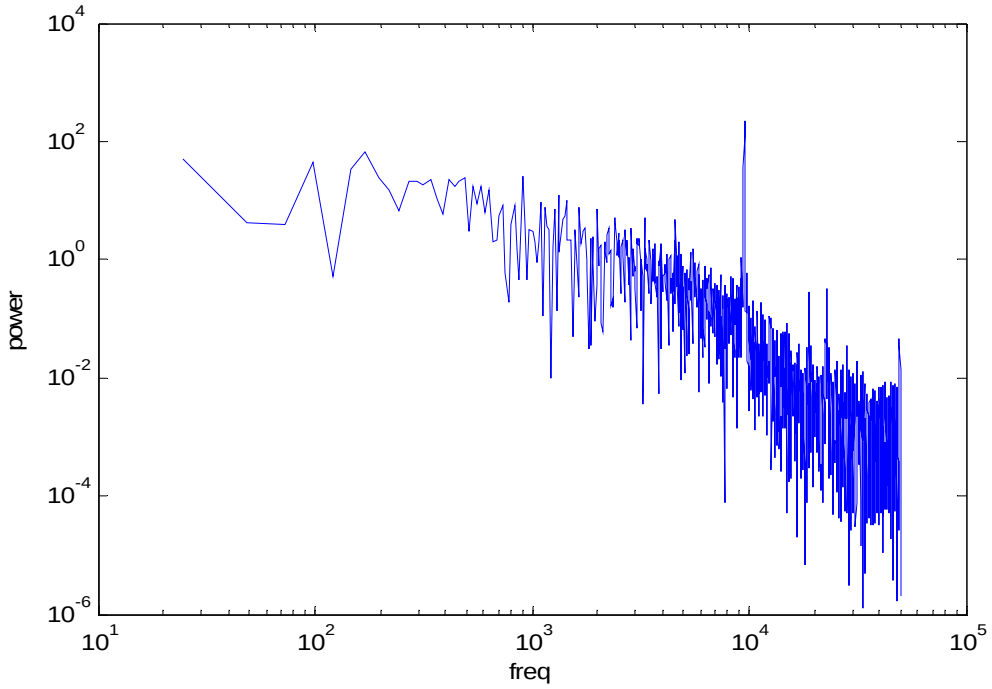

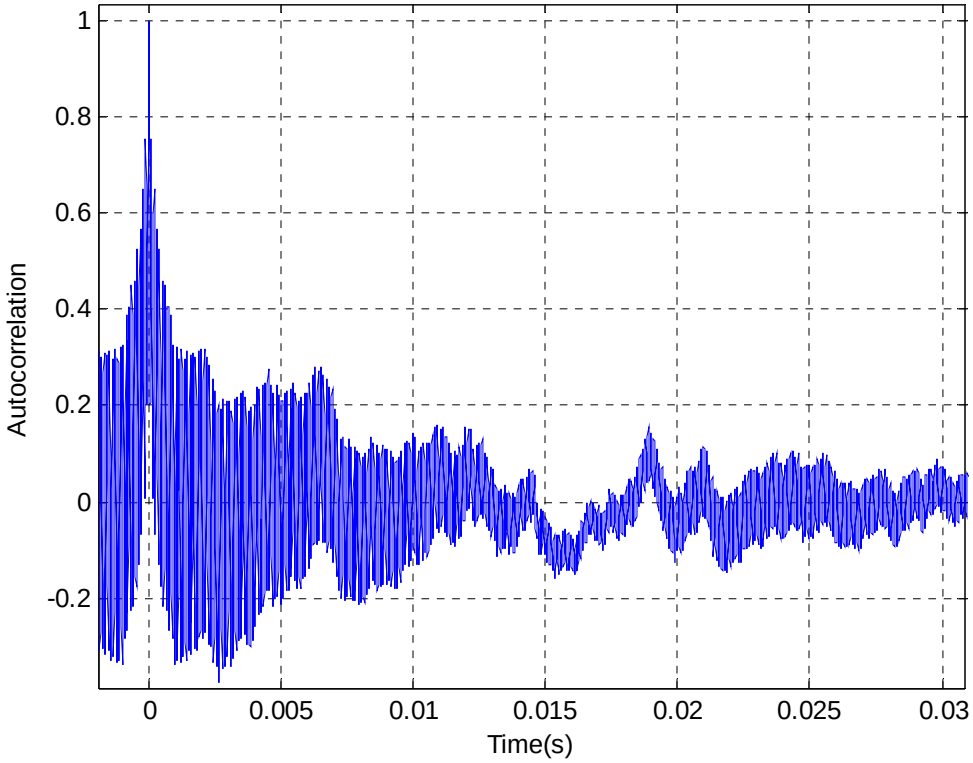
Autocorrelation
1
0.8
0.6
0.4
0.2
0
-0.2
0
0.005
0.01
0.015
0.02
0.025
0.03
Time(s)

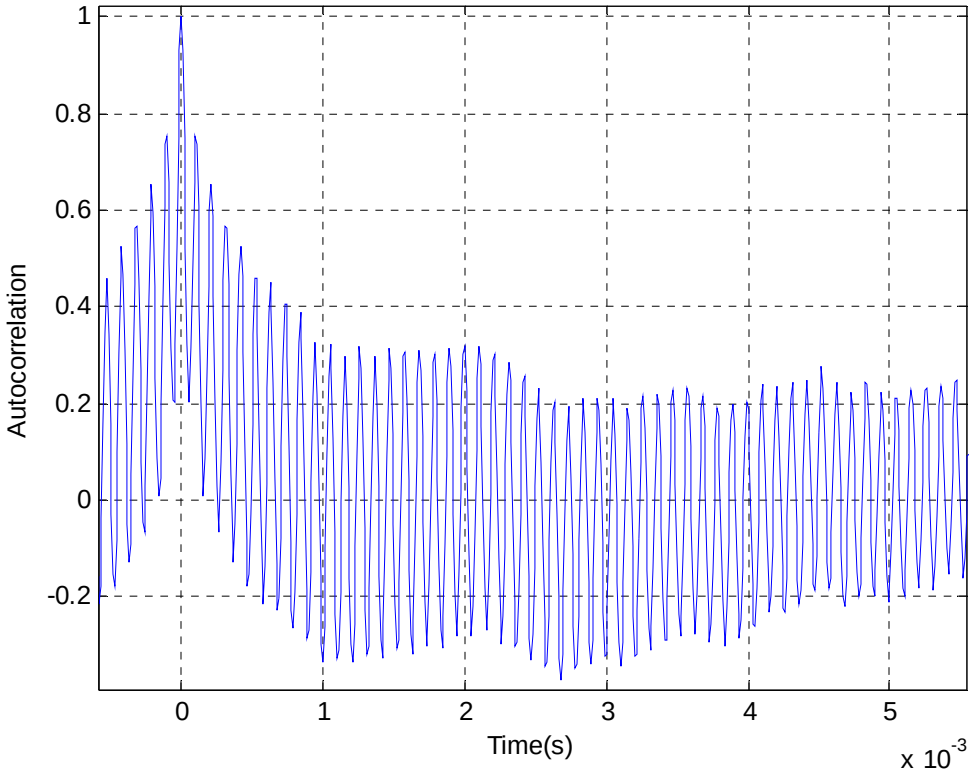
Autocorrelation
1
0.8
0.6
0.4
0.2
0
-0.2
0
1
2
3
4
5
Time(s)
x 10-3

APPENDIX E: 70 PERCENT SPEED STEAM INDUCED STALL: HOT-FILM DATA

Hot-film velocity trace from the IFA 100 and processed using MATLAB program from Appendix B

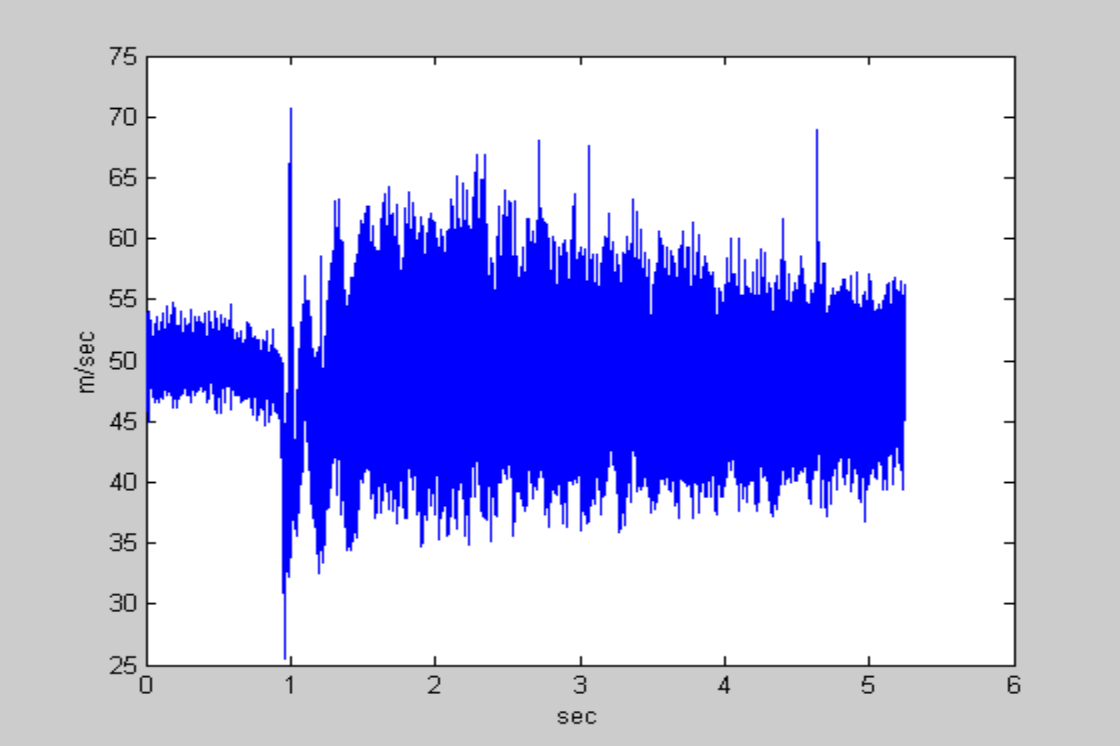

THIS PAGE INTENTIONALLY LEFT BLANK

APPENDIX F: 70 PERCENT SPEED STEAM INGESTION WITHOUT STALL: HOT-FILM DATA

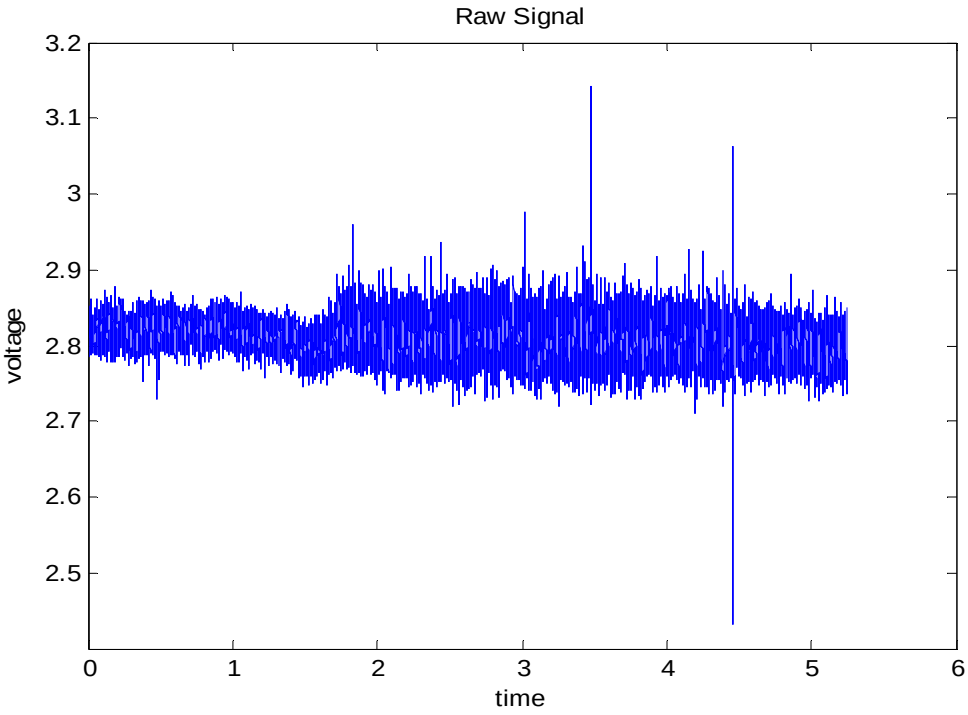

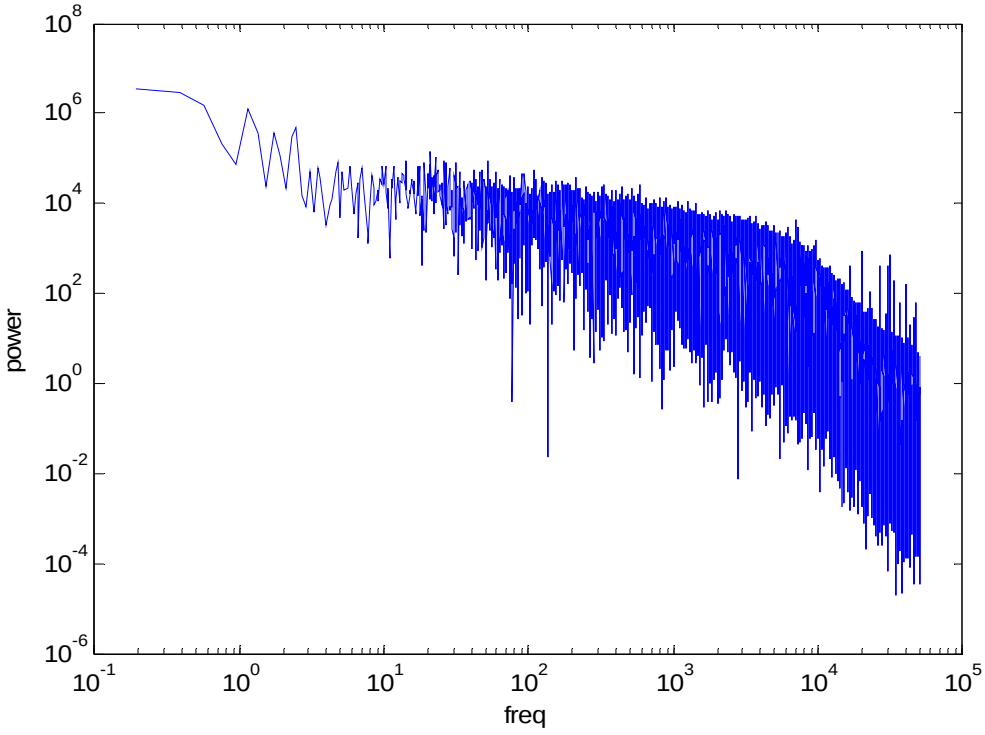

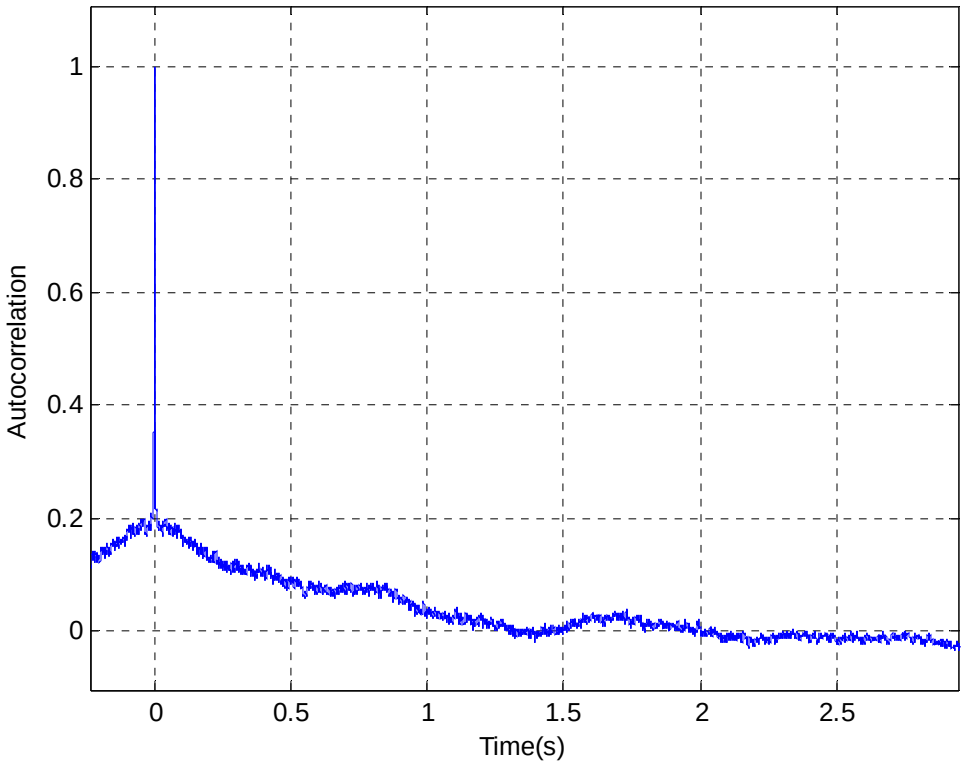
Autocorrelation
Time(s)
0
0.2
0.4
0.6
0.8
1
0.5
1.5
2
2.5

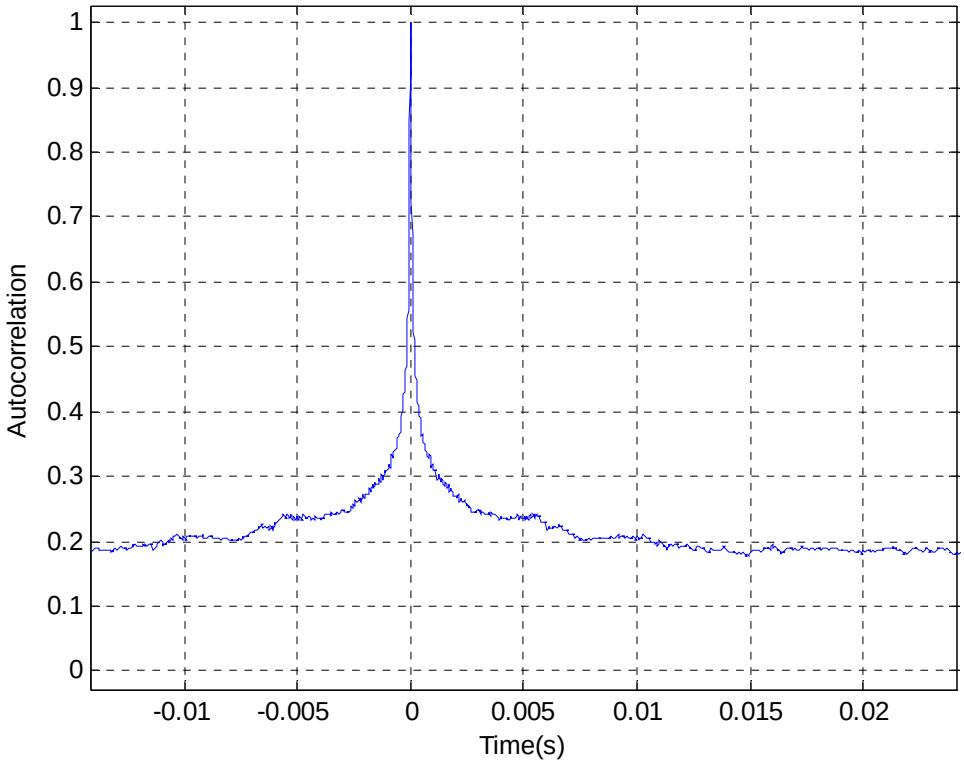
Autocorrelation
Time(s)
0
0.1
0.2
0.3
0.4
0.5
0.6
0.7
0.8
0.9
1
-0.01
-0.005
0.005
0.01
0.015
0.02

INITIAL DISTRIBUTION LIST

1. Defense Technical Information Center
   Ft. Belvoir, Virginia

2. Dudley Knox Library
   Naval Postgraduate School
   Monterey, California

3. Distinguished Professor and Chairman Anthony Healey
   Department of Mechanical and Aeronautical Engineering
   Naval Postgraduate School
   Monterey, California

4. Professor Raymond Shreeve
   Department of Mechanical and Aeronautical Engineering
   Naval Postgraduate School
   Monterey, California

5. Professor Garth Hobson
   Department of Mechanical and Aeronautical Engineering
   Naval Postgraduate School
   Monterey, California

6. Dr. Anthony Gannon
   Department of Mechanical and Aeronautical Engineering
   Naval Postgraduate School
   Monterey, California

7. Naval Air Warfare Center
   Propulsion and Power Engineering
   ATTN: Mark Klien
   Patuxent River, Maryland

8. LT Thomas Payne
   Monterey, California